

UNIVERZITA KARLOVA V PRAZE

Přírodovědecká fakulta

Studijní program: Chemie

Studijní obor: Chemie životního prostředí



Bc. Jaroslav Smitka

STUDIE INKLUZNÍCH KOMPLEXŮ PESTICIDŮ
S KUKURBITURILY

Study of inclusion complexes of pesticides with cucurbiturils

Diplomová práce

Vedoucí diplomové práce: prof. RNDr. Eva Tesařová, CSc.

Konzultant: Professor Doutor José Paulo da Silva

Praha 2013

This work was carried out in collaboration with Professor Doutor José Paulo da Silva under the Erasmus program at University of Algarve in Faro, Portugal.

Prohlášení

Prohlašuji, že jsem tuto závěrečnou práci zpracoval samostatně a že jsem uvedl všechny použité informační zdroje a literaturu. Tato práce ani její podstatná část nebyla předložena k získání jiného nebo stejného akademického titulu.

Jsem si vědom toho, že případné využití výsledků, získaných v této práci, mimo Univerzitu Karlovu v Praze je možné pouze po písemném souhlasu této univerzity.

V Praze dne 10. května 2013.

Jaroslav Smitka

Acknowledgment

My many thanks belong to prof. RNDr. Eva Tesařová, CSc. and Professor José Paulo da Silva for their expert supervision, valuable advises and comments, effort made while giving me the information, inspiration, and availability.

Klíčová slova:

Pesticidy

Inkluze

Kukurbiturily

Cyklodextriny

Vysokoúčinná kapalinová chromatografie

Hmotnostní spektrometrie

UV/VIS spektroskopie

Key words:

Pesticides

Inclusion

Cucurbiturils

Cyclodextrins

High performance liquid chromatography

Mass spectrometry

UV/VIS spectroscopy

Abstrakt

Výsledky v této diplomové práci se týkají formování inkluzních komplexů pesticidů, konkrétně kyseliny 1-naftyloctové, 1-naftylacetamidu, karbarylu a napropamidu, s kukurbiturily a pro srovnání též s cyclodextriny. Bylo sledováno, jak komplexace pesticidů s inkluzními sloučeninami může ovlivnit jejich fotodekompozici. Pro studium formování inkluzních komplexů byla zvolena hmotnostní spektrometrie, kapalinová chromatografie ve spojení s hmotnostním detektorem i spektrofotometrickým detektorem a spektrofotometrie v UV oblasti spektra. Hmotnostní spektrometrie umožnila objasnění stechiometrií studovaných komplexů. Ostatní metody poskytly informace o fotochemii studovaných látek.

Kukurbiturily a jejich komplexy s pesticidy jsou ionizací elektrosprejem (hmotnostní spektrometrie) snadno detekovatelné v plynné fázi, kde se primárně objevují jako nabitě ionty, obsahující H^+ , Na^+ či K^+ . Vyhodnocení bylo provedeno na základě hodnot m/z signálu a posléze potvrzeno fragmentací (tandemová hmotnostní spektrometrie). Všechny studované pesticidy tvoří komplexy s kukurbiturily v poměru 1:1 případně i 1:2 (hostitel:analyt). Výjimku tvoří kyselina 1-naftyloctová, která formuje pouze komplexy v poměru 1:1.

Rychlostní konstanty fotorozkladu byly zjištěny za použití HPLC a spektrofotometrie. Výsledky ukazují, že je-li komplex vystavený UV záření, cyclodextrin stabilizuje daný pesticid mnohem efektivněji než komplex s kukurbiturily. Obecně lze říci, že nejrychleji se rozkládá neinkludovaná forma analytu, o něco málo pomaleji komplex s kukurbiturilem, a nakonec pesticid komplexovaný s cyclodextrinem.

Abstract

In this work we report the formation of inclusion complexes of the pesticides 1-naphthylacetic acid, 1-naphthylacetamide, napropamide and carbaryl with cucurbit[n]uril (n=7 and 8) and β -cyclodextrin hosts. We also report results of the photochemistry of these compounds when free in aqueous solution and included within these nano-containers. The formation of inclusion complexes was studied by electrospray ionization mass spectrometry (ESI-MS) which gave us information about stoichiometry of the complexes and about their reactivity in the gas phase. The photodecomposition and formation of products was followed by high performance liquid chromatography coupled to both mass spectrometry (HPLC-MS) and UV/VIS detector, and spectrophotometry.

The studied CBs and their host-guest complexes were readily detected in the gas phase by ESI-MS, mainly as single and double charged ions containing either H^+ , Na^+ or K^+ . The assignments were made based on the m/z values of the observed signals and further confirmed by fragmentation (tandem mass spectrometry – MS^n). All pesticides formed 1:1 (host:guest) complexes. Carbaryl, napropamide and 1-naphthylacetamide also formed 1:2 (host:guest) complexes. Under some solution chemistry conditions, namely for concentrations of cucurbiturils above $50 \mu M$ and at low acid and salt concentrations ($< 10^{-5} M$) aggregates could also be observed.

Most of the studied pesticides undergo photodegradation when free in solution. Several unknown photoproducts were observed, namely with $m/z = 232$ for 1-naphthylacetamide@CB[8] and $m/z = 218, 240, 329$ for 1-naphthylacetamide@CB[7]. Further studies using other techniques, namely GC-MS, or HPLC-MS/MS are needed to assign a structure to the photoproducts.

Spectrophotometry as well as HPLC clarifies the photodegradation process of studied pesticides. Rate of decomposition constants explain the photodecomposition of each pesticide when free and included within a host. It seems that cyclodextrin includes the pesticides more efficiently than cucurbiturils. This result in faster photodegradation of non-included compounds, followed by analytes included into complex of cucurbituril, and then those forming inclusion complexes with cyclodextrin.

List of abbreviations

ACN	acetonitrile
APCI	atmospheric pressure chemical ionization
APPI	atmospheric pressure photoionization
Carb	carbaryl
CB	cucurbituril
CD	cyclodextrin
CD-G	inclusion complex of cyclodextrin with pesticide
CI	chemical ionization
DC	direct current
EI	electron impact
ELISA	enzyme-linked immunoassay
ESI-MS	electrospray ionization mass spectrometry
G	guest
GC-MS	gas chromatography – mass spectrometry
HILIC	hydrophilic interaction liquid chromatography
HPLC	high performance liquid chromatography
ICR	ion cyclotron resonance
k	retention factor
k_x	rate constant
K	stability constant
LC-MS	liquid chromatography – mass spectrometry
m/z	mass-to-charge ratio
MeOH	methanol
MS	mass spectrometry
MS/MS	tandem mass spectrometry
NAAc	1-naphthylacetic acid
NAAm	1-naphthylacetamide
NAP	napropamide
NP-HPLC	normal phase high performance liquid chromatography
Q	quadrupole
QIT	quadrupole ion trap

R	correlation coefficient
R _{1,2}	resolutions
RF	radio frequency
RP-HPLC	reverse phase high performance liquid chromatography
RTP	room temperature phosphorescence
S	solubility
SFC	supercritical fluid chromatography
t _M	dead time
TOF	time of flight
t _R	retention time
UV/VIS	ultraviolet and visible region of spectra
v/v	volume ratio

Index

Acknowledgment	- 3 -
Klíčová slova:	- 4 -
Key words:	- 4 -
Abstrakt.....	- 5 -
Abstract.....	- 5 -
List of abbreviations	- 7 -
Index	- 9 -
1 Introduction.....	- 11 -
2 Theory.....	- 12 -
2.1 Host-guest molecules	- 12 -
2.1.1 Cyclodextrins.....	- 12 -
2.1.2 The cucurbit[n]uril family.....	- 16 -
2.2 Photochemistry	- 21 -
2.3 Analysis methods	- 23 -
2.3.1 Mass spectrometry	- 23 -
2.3.1.1 Ion sources	- 24 -
2.3.1.2 Mass analyzers	- 24 -
2.3.1.3 Detector - ion analysis	- 25 -
2.3.1.4 Tandem mass spectrometry.....	- 25 -
2.3.2 Chromatographic methods	- 25 -
2.3.2.1 High performance liquid chromatography.....	- 26 -
2.3.2.1.1 HPLC detectors	- 26 -
2.3.2.1.2 Processing of measured data	- 27 -
2.4 Studied pesticides.....	- 28 -
3 Objectives.....	- 32 -
4 Experimental part	- 33 -
4.1 Solvents	- 33 -
4.2 Organic compounds	- 33 -
4.3 Equipment.....	- 33 -
4.4 Sample preparation.....	- 34 -
4.5 Sample irradiation	- 35 -

4.6	Measurement conditions.....	- 35 -
4.6.1	Mass spectrometer	- 35 -
4.6.2	Liquid chromatograph.....	- 35 -
4.6.3	Spectrophotometer.....	- 36 -
5	Results and discussion	- 37 -
5.1	ESI-MS.....	- 37 -
5.2	LC-MS.....	- 42 -
5.3	Spectrophotometry	- 43 -
5.3.1	Pesticide spectra	- 43 -
5.3.2	Rate constants determination.....	- 46 -
5.4	HPLC.....	- 51 -
5.4.1	Pesticide analysis	- 51 -
5.4.2	Rate constant determination	- 53 -
6	Conclusions	- 60 -
	References.....	- 61 -

1 Introduction

Cucurbiturils can be categorized to the same group of molecular containers as cyclodextrins. Although both compounds are capable of encapsulating other, smaller substances general properties and use differ in some aspects and use. It is known that cyclodextrins have huge potential as drug carriers, the cucurbiturils are, however, more used in nanotechnology.

Pesticides are well-known for their effect on various targets. Thus, the complexation of cucurbiturils and cyclodextrins (hosts) with these pesticides (guests) may lead to possible extension of use of these agricultural substances. One could expect that the inclusion process will affect the stability of the pesticides; particularly it can protect the compound from rapid decomposition, when exposed to light. For observing the possible degradation products, it is useful to use techniques such as electrospray ionization mass spectrometry or high performance liquid chromatography.

2 Theory

2.1 Host-guest molecules

Molecular containers are hollow rigid organic host compounds. Their interior cavities are sufficiently large to include small guest molecules. Generally they have macrocyclic structures with openings of different sizes that allow the guest to enter and exit. Rebek and co-workers have reported that self complementary molecules can undergo dimerization in order to form spherical capsules in which smaller guest may be included. Also the encapsulation process as well as the release of the guest can be controlled by the change in the medium acidity [1], type of buffer and its concentration, temperature, and added organic solvent [2].

The inclusion of guest molecules into cavities of supramolecular hosts with molecular container properties has a great potential to mimic enzymatic activity, to isolate reactive species, to promote uncommon spectroscopic effects and to allow novel chemical transformations. There are several molecular container hosts such as cyclodextrins (CDs), calixarenes or cucurbiturils (CBs) that allow a fast exchange of the guest as their openings are unobstructed [3]. Cyclodextrins, products of the reaction of an enzyme cyclodextrinase and starch, are natural compounds, whereas cucurbiturils are synthetically tailored [4]. As cyclodextrins are perhaps the most explored inclusion compounds, they seem to have quite important role due to following reasons: 1) they are produced from a starch by relatively simple enzymatic reaction, 2) because they are able to form inclusion complexes, the complexed substances can be modified significantly, 3) any eventual caused toxicity is of secondary character and can be ousted by choosing a proper cyclodextrin or its derivative and thus humans can consume cyclodextrins as a part of food, drug or cosmetics [5].

2.1.1 Cyclodextrins

First reference to cyclodextrin appeared in 1891 when Villiers isolated 3 g of a crystalline substance from 1000 g of starch. He named this substance cellulose. Villiers, however, was convinced that the enzymatic reaction took place at presence of *Bacillus amylobacter* which probably was not entirely pure culture but also contained *Bacillus macerans*. He also pointed out that two forms of celluloses were formed, perhaps α -CD and β -CD. Several years later, Schardinger, a scientist studying bacteria that survived during cooking process, concluded that digesting starch with such a microorganism led to

two different crystalline products, which were described with regard to their lack of reducing power. They appeared to be quite similar to Villiers products. The isolated microbe, capable of producing acetone and ethyl alcohol from sugar and starch-containing plant material, was named *Bacillus macerans*. Furthermore, he reported that several adducts are created while iodide solution was added. Iodine was the main factor in distinguishing between α -dextrin and β -dextrin. In 1930s, Freudenberg and co-workers concluded that Schardinger dextrins are comprised of maltose units and contain only α -1,4-glycosidic linkages. Later, in 1936, the first cyclic structure of these crystalline dextrins was described. The γ -CD had been discovered and described 12 years later due to X-ray crystallography. All of that was followed by recognition that CDs can form inclusion complexes [5,6].

Cyclodextrin family consists of three parent cyclodextrins (first generation) α -CD, β -CD, and γ -CD which are composed of six, seven, and eight glucose units, respectively [6,7]. These structures can be seen in Fig. 1.

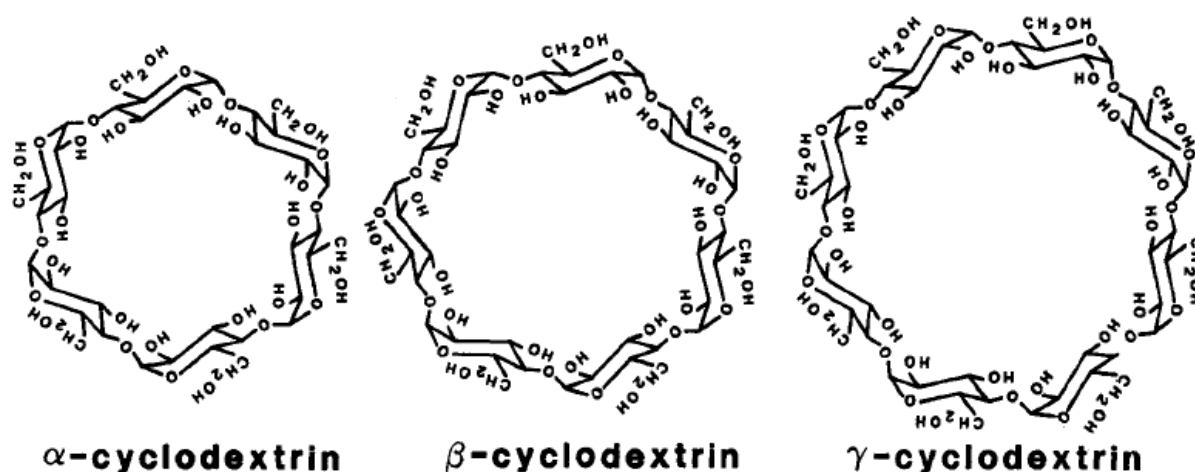


Figure 1 Structure of α -, β -, γ - cyclodextrins [7].

The three major cyclodextrins are crystalline, homogenous, nonhygroscopic substances that are torus-like macro-rings [5]. Other cyclodextrins were also isolated such as δ -CD. The stability, however, was quite low while the solubility was too high (in general the isolation is also complicated). Moreover, the larger CDs do not share the regular cylinder shape as they are collapsed and their real cavity is even smaller than of the γ -CD. Cyclodextrins that contain less than 6 glucose residues are too strained to exist [5,8]. Besides the natural cyclodextrins, various derivatives have been produced. Typically, they

are synthesized by aminations, esterifications or etherifications of primary and secondary hydroxyl groups of the cyclodextrin. Based on a substituent, the solubility of a derivative is usually different from parent cyclodextrin. All derivatives have changed hydrophobic cavity size which contributes to better solubility, stability against light or oxygen and also helps to control the chemical activity of guest molecules [6]. X-ray structures show that in cyclodextrins the secondary hydroxyl groups (C_2 and C_3) are located on the wider edge of the ring and the primary hydroxyl groups (C_6) on the other edge, and the apolar C_3 and C_5 hydrogens and ether-like oxygens are at the inside of the torus-like molecules. As a result we get a molecule where the outside is hydrophilic capable of dissolving in water and a hydrophobic cavity. The cavity thus provides an environment where wide range of hydrophobic smaller substrates can be entrapped. Molecular dimensions of common cyclodextrins and functional structural scheme of β -cyclodextrin are shown in Fig. 2 and Fig. 3, respectively.

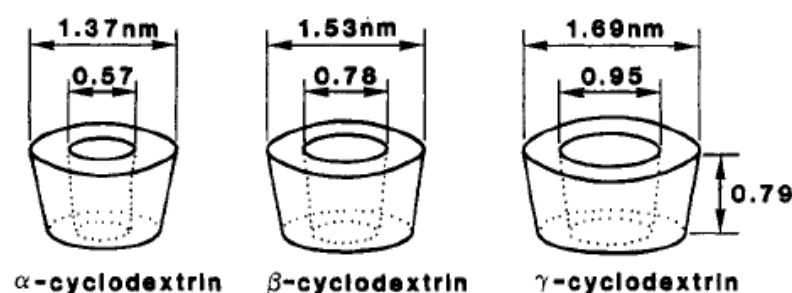


Figure 2 Molecular dimensions of cyclodextrin [7]

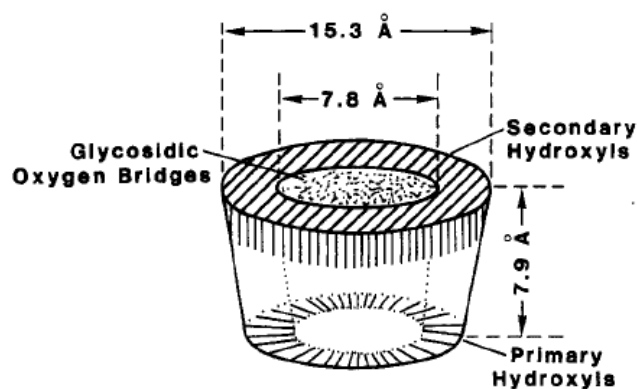


Figure 3 Functional structural scheme of β -cyclodextrin [7]

Cyclodextrins have at their disposal one of the most interesting features. They have the ability to form inclusion complexes (host-guest complexes) with a great variety of solid, liquid and gaseous compounds by molecular complexation. In these complexes, lipophilic cavity of cyclodextrin hosts a guest molecule. As the formation of inclusion complexes takes place, no covalent bonds are formed, nor destroyed. The forming force is provided by the release of enthalpy rich water molecules from the cavity. Water molecules are dislocated by more hydrophobic guest molecules present in the solution to achieve an apolar-apolar association and decrease of cyclodextrin ring strain resulting in a more stable lower energy state [6]. Despite the fact that the most frequent host-guest ratio is 1:1, other aggregates have been observed such as 2:1, 1:2. Even more complicated associates have been formed. The host-guest complexes can be isolated as stable crystalline substances. As the complexes dissolve, equilibrium is established between dissociated and associated species which can be formulated by stability constant K_a [5]. This equilibrium is illustrated in equation 1 [7], where CD represents a cyclodextrin and G figures as a guest molecule and CD-G is the inclusion complex.



The inclusion complex stability constant is described by equation 2 [7]:

$$K_a = [CD-G] / ([CD] \cdot [G]) \quad (2)$$

The binding forces in the complex formation are 1) van der Waals interactions (or hydrophobic interaction) between the hydrophobic specie of the guest molecules and the cyclodextrin cavity, 2) hydrogen bonding between the polar functional groups of guest molecules and the hydroxyl groups of cyclodextrin, 3) release of high energy water molecules from the cavity in the formation process, and 4) release of strain energy in the ring frame system of cyclodextrin. Concerning the stability of the inclusion complexes, the medium, temperature, and the polarity of guest molecules are the most important factors. The geometric shape also has to be taken into an account as for example too small guests will enter and exit the host freely with little or no bonding at all. Larger molecules than is the cavity diameter, however, can bind with certain groups or their hydrophobic side chains can penetrate into the cyclodextrin cavity. Another aspect is that only substances

less polar than water can form an inclusion complex with cyclodextrins. When the formation of inclusion complexes is intended, the temperature should be watched as rising temperature affects negatively the stability of an inclusion complex [7].

The ability of cyclodextrin to encapsulate many organic compounds aids to improve many of their special characteristics such as 1) improving the solubility of the molecule in the presence of light, heat and oxidizing conditions, 2) decreasing volatility of the compound, 3) masking of ill smell and taste, and 4) masking pigments or the color of the substances. As a result, the cyclodextrins have been used in many industrial fields such as cosmetics, personal care, toiletry, foods and flavors pharmaceuticals as well as in agricultural and chemical industries. The great importance also lays upon wider applications of cyclodextrins in chromatographic techniques [6] and drug carrier systems [9].

2.1.2 The cucurbit[n]uril family

Cucurbit[n]uril (CB) is a family of macrocyclic host molecules composed of glycoluril units linked by a pair of methylene groups. It has been over 100 years since Behrend *et al.* reported that the condensation of glycoluril (acetylenurea) and formaldehyde in concentrated HCl yields an insoluble polymeric substance that is nowadays known as Behrend's polymer [10]. Behrend *et al.* recrystallized the product from concentrated H₂SO₄, which led to a crystalline substance in good yield (40 – 70%), and presented the formed complexes (cocrystals) with various substances such as KMnO₄, AgNO₃, H₂PtCl₆, congo red or methylene blue. It took until 1981 to decipher its chemical nature and structure when Mock and co-workers reported the parent compound cucurbit[6]uril, macrocyclic structure comprising six glycoluril units and twelve methylene bridges. The name cucurbituril is derived from the *cucurbitaceae* family due to its pumpkin shape [10]. In 2000, scientific groups of Kim and Day carried out a X-ray crystallography that resulted in discovery of three new CB[n] homologues (CB[5], CB[7], CB[8] [10,11,12], and a macrocycle within a macrocycle CB[5]@CB[10] (smaller CB[5] lies inside of larger CB[10]). Day and co-workers also attempted to remove CB[5] from the cavity of CB[10]. The isolation, however, has not been successful. The structures of the main homologues are shown in Fig. 4 [13].

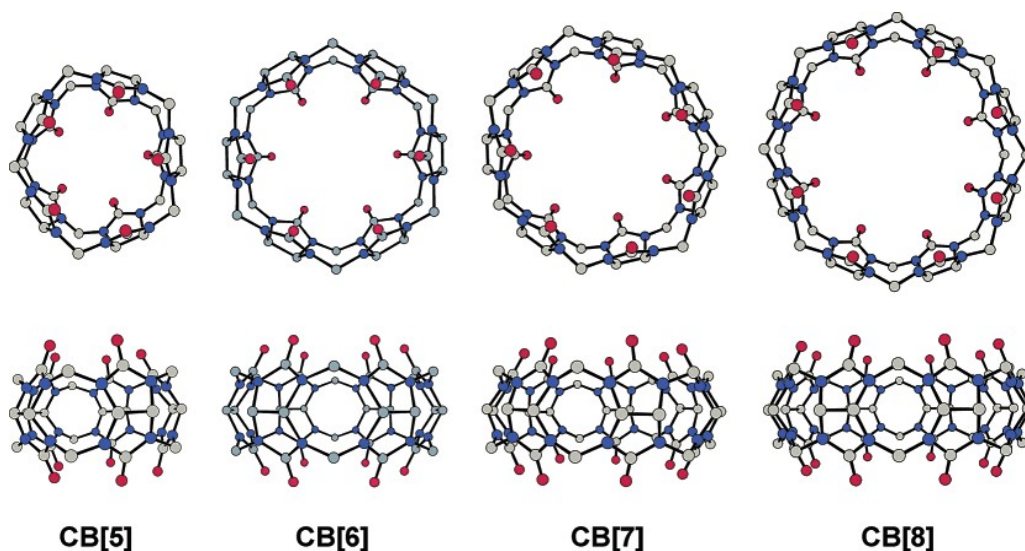


Figure 4 X-ray crystal structures (top and side view) of cucurbit[n]urils ($n = 5 - 8$). Atoms are illustrated as follows: grey/carbon, red/oxygen and blue/nitrogen [13].

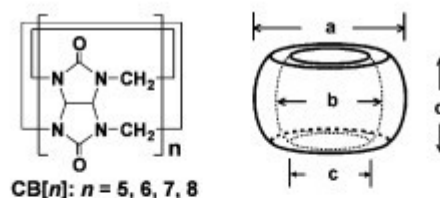
The compound cucurbit[6]uril has a hydrophobic cavity of ~ 5.5 Å diameter and two identical carbonyl-laced portals of ~ 4 Å diameter. Even though the cavity size is quite similar to α -cyclodextrin, the highly symmetrical structure of cucurbit[6]uril with two identical openings differs from α -CD. As the polar ureido carbonyl groups at the portals are very likely to bind ions and molecules through charge-dipole and hydrogen bonding interactions, the hydrophobic groups carry a great potential to pair with nonpolar character (similar to CDs). Cucurbiturils, however, are very fond of forming very stable inclusion complexes with a great variety of alkyl- and aryl- amines (unlike CDs). The CBs regions around carbonyl oxygens as well as the internal part of the cavity are quite negative but the outer surface is positive. On the other hand, the portal and the cavity of CDs are nearly hydrophobic [11]. In spite of its preference to bind positively charged guests, CB[6] interacts more strongly with alcohols (besides hexanol) than does α -CD. In general, CB[6] seems to bind its guests with higher selectivity and affinity than the cyclodextrin.

As the CB[7] is more voluminous it can interact with more structurally different and bigger guests than CB[6]. It binds a great variety of aromatic substances such as naphthalene, stilbene, ferrocene, adamantanes or bicyclooctanes. Concerning the cavity volume CB[8] resembles γ -cyclodextrin but the conformation flexibility of CB[8] is lower. Similarly to CB[n] ($n = 5-7$) CB[8] preferably binds positively charged guests by ion-dipole interactions. The single guest can be bound either partially or fully filling the cavity. Unlike CB[n] ($n = 5-7$), the cavity of CB[8] has the ability to simultaneously bind two

aromatic rings [10].

Some structural properties of the above mentioned cucurbit[n]urils ($n = 5-8$) are compared in Tab. 1.

Table 1 Comparison of structural parameters of CB homologues [13].



		CB[5]	CB[6]	CB[7]	CB[8]
outer diameter (Å)	a	13.1	14.4	16.0	17.5
cavity (Å)	b	4.4	5.8	7.3	8.8
	c	2.4	3.9	5.4	6.9
height (Å)	d	9.1	9.1	9.1	9.1

The CB[6] chemistry from its early days was struck by many issues such as poor solubility in aqueous and organic solutions, a lack of homologous series of different sized hosts, and an inability to access CB[n] derivatives and analogues by tailor-made synthetic procedures. All of these early difficulties passed with new millennium. The CB[n] family currently provides a great potential in nanotechnology as components of molecular machines due to its special properties: 1) high binding selectivity, 2) binding interactions of high affinity, 3) synthetic control over size, shape, and functional group placement, 4) great structural integrity, 5) association and dissociation with controlled kinetics, and 6) control of the molecular recognition processes by suitable electrochemical, photochemical, and chemical approaches [10].

Poor solubility of CB[n] in common solvents is a major limitation of these compounds, mainly CB[6] ($S_{H_2O} = 0.018$ mM) and CB[8] ($S_{H_2O} = < 0.01$ mM). CB[5] ($S_{H_2O} = 20 - 30$ mM) and CB[7] ($S_{H_2O} = 20 - 30$ mM) are moderately soluble in water. Their solubility is comparable with that of β -cyclodextrin ($S_{H_2O} = 16$ mM), the least soluble compound of the family of cyclodextrins. Generally the solubility of CBs is lower than that of cyclodextrins [10,11]. Higher solubility of CB[7] has a significant beneficial effect on fluorescent dyes increasing their fluorescence intensity, solubilization and disaggregation, enhancing their

photostability and providing some protection against fluorescence quenchers [4]. The CB[n] also possesses a great thermal stability as no decomposition has been observed up to 420 °C for CB[n] (n = 5, 6, 8). Cucurbit[7]uril, however, decomposes at lower temperature of 370 °C. Some of the discussed physical properties of cucurbit[n]urils and cyclodextrins are compared in Table 2.

Table 2 Physical properties and dimensions of CB[n] and CDs [10].

	M_r	a [Å]	b [Å]	c [Å]	V [Å ³]	s_{H_2O} [mM]	Stability [°C]	pK _a
CB[5]	830	2.4	4.4	9.1	82	20–30	>420	
CB[6]	996	3.9	5.8	9.1	164	0.018	425	3.02
CB[7]	1163	5.4	7.3	9.1	279	20–30	370	
CB[8]	1329	6.9	8.8	9.1	479	<0.01	>420	
CB[10] ^[b]	1661	9.0–11.0	10.7–12.6	9.1	–	–	–	–
α-CD	972	4.7	5.3	7.9	174	149	297	12.332
β-CD	1135	6.0	6.5	7.9	262	16	314	12.202
γ-CD	1297	7.5	8.3	7.9	427	178	293	12.081

M_r – molecular weight; a, b, c – structural parameters from Fig. 5, V – volume, S – solubility, pK_a – acidity constant

To sum up the formation of host-guest complexes, we can say that CBs and CDs bind similarly sized molecules related to the number of units connected together and thus the cavity size. These host families, however, differ from each other in host-guest interactions caused by the different functional groups around the entrance of the cavity. The CD cavity contains the OH groups which results in hydrogen bonding of the guest. Carbonyl groups, however, are present at the portal of CBs so the charge-dipole interactions as well as hydrogen bonding with guests may take place. These groups also have the ability to coordinate with metal ions [13]. My colleague, Magda Ördögová, has carried out a study in which she aimed to determine the interactions of cucurbit[7]uril and selected cyclodextrins with 1-naphthylacetic acid and 1-naphthylacetamide by capillary electrophoresis [14]. She managed to determine stability constants for β-cyclodextrin, γ-cyclodextrin, and 6-monodeoxy-6-monoamino-β-CD (MA-β-CD) [14]. These constants are presented in Table 3.

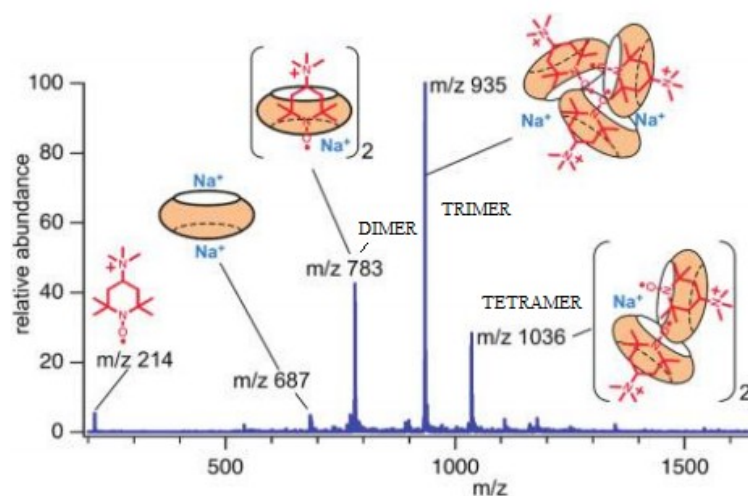
Table 3 Stability constants of selected host-guest molecules [14].

Guest	Host	Stability constant K	SD
1-naphthylacetic acid	β -CD	0.039	± 0.0012
	γ -CD	0.026	± 0.0013
	MA- β -CD	0.073	± 0.0031
1-naphthylacetamide	MA- β -CD	0.07	± 0.0034

These results suggest that, concerning neutral cyclodextrins, 1-naphthylacetic acid interacts more strongly with β -CD. However, the strongest inclusion was observed of both 1-naphthylacetamide and 1-naphthylacetic acid into MA- β -CD. CBs did not seem to have any interaction with measure pesticides [14].

Da Silva and co-workers have recently conducted a study using electrospray ionization mass spectrometry (ESI-MS) proving its important role in observing free cucurbiturils and their host-guest complexes and other noncovalent systems. The complexes are transformed into the gas phase intact. Complexes between CBn and several ionic and neutral guests have been studied giving an important information including the nature and stoichiometry of the complexes, their binding constants, and also their reactivity in the gas phase (see Fig. 5) [15].

It is obvious that CB[8] undergoes di-, tri-, and even tetramerization. This fact can complicate the study of inclusion complexation and determination of stability constants.

**Figure 5** ESI-MS spectrum of CB[8] aggregates [15].

2.2 Photochemistry

Molecular photochemistry is a science describing physical and chemical processes that are induced by photons, in terms of a concrete mechanistic model based on molecular structures and their implied properties.

The photoreaction is initiated by the light absorption. This confers to photoreactions selectivity and the ability to initiate reactions at very low temperatures (photoreactions close to the temperature of 0 K have been reported) [16]. Grotthus and Draper formulated the first law of photochemistry at the beginning of 19th century stating that the light must be absorbed by a molecule so that the photochemical reaction can take place [17]. The Lambert-Beer law implies that absorption of radiation shall be treated quantitatively. The fraction of monochromatic light transmitted through an absorbing system can be expressed as follows:

$$\frac{I_t}{I_0} = 10^{-\epsilon Cd} = e^{-\alpha Cd} \quad (3)$$

where I_t and I_0 are transmitted and incident light intensities, respectively. C is the concentration of absorber, d is the optical path. ϵ is the decadic absorption coefficient (which depends on the wavelength of radiation) and α represents molar absorption coefficient. The arrangement of photochemical reaction is depicted in Fig. 6. The relationship follows naturally from the assumption that the rate of loss of photons is proportional to the rate of bimolecular collisions between photons and the absorbing species. The Beer-Lambert law is of particular importance in determining the intensity of absorbed radiation in photochemical experimentation, and in calculating concentrations from absorption measurements [17,18].

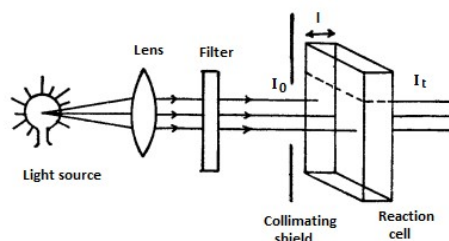


Figure 6 Optical arrangement for photochemical reactions [19].

Photophysical processes may be defined as transitions which interconvert excited states or excited states into the ground state. No chemistry is therefore involved. The important photophysical processes can be classified as radiative and radiationless. Fig. 7 represents a scheme showing photophysical radiative processes, radiationless processes and photochemical processes.

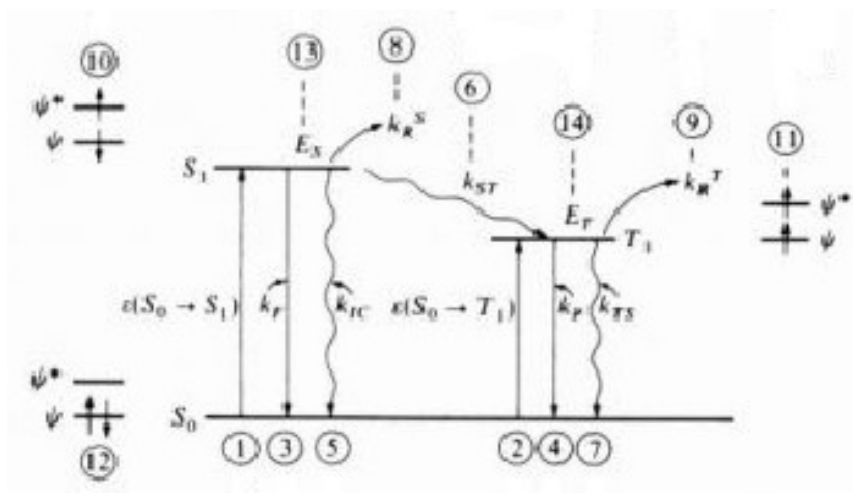


Figure 7 State energy diagram [16].

Radiative processes shown in the Fig. 10 are [taken from 16]:

- 1) Singlet-singlet absorption ($S_0 + h\nu \rightarrow S_1$), characterized experimentally by an extinction coefficient $\epsilon(S_0 \rightarrow S_1)$;
- 2) Singlet-triplet absorption characterized ($S_0 + h\nu \rightarrow T_1$), characterized experimentally by an extinction coefficient $\epsilon(S_0 \rightarrow T_1)$;
- 3) Singlet-singlet emission called fluorescence ($S_1 \rightarrow S_0 + h\nu$), characterized by a radiative rate constant k_f ;
- 4) Triplet-singlet emission called phosphorescence ($T_1 \rightarrow S_0 + h\nu$), characterized by radiative rate constant k_p .

The photophysical radiationless processes are:

- 5) “Allowed” transitions between states of the same spin called internal conversion (e.g., $S_1 \rightarrow S_0 + \text{heat}$), characterized by a rate constant k_{IC} ;
- 6) “Forbidden” transitions between excited states of different spin called intersystem crossing (e.g., $S_1 \rightarrow T_1 + \text{heat}$), characterized by a rate constant, k_{ST} ;
- 7) “Forbidden transitions” between triplet states and the ground state – also called intersystem crossing (e.g., $T_1 \rightarrow S_0 + \text{heat}$), characterized by a rate constant, k_{TS} .

The photochemical processes may be defined as transitions from an electronically excited state to yield structures that differ in constitution or configuration from S_0 . Such processes are:

- 8) Singlet reaction, characterized by a rate constant k_R^S ;
- 9) Triplet reaction, characterized by a rate constant k_R^T .

The configurations and energies are:

- 10) Singlet orbital configuration;
- 11) Triplet orbital configuration;
- 12) Ground state orbital configuration;
- 13) Singlet energy;
- 14) Triplet energy

2.3 Analysis methods

Inclusion complexes can be analyzed, as proposed by various research groups in the literature [10], by numerous methods.

For our purposes, we decided to use mass spectrometry (MS), liquid chromatography hyphenated with mass spectrometry (LC-MS), UV/VIS spectrometry, and high performance liquid chromatography (HPLC).

2.3.1 Mass spectrometry

Mass spectrometry is a modern highly efficient, analytical technique for “weighing” individual molecules. The molecules are converted into ions in vacuum, submitted to electric and magnetic fields, and their consequent trajectories measured to obtain the mass-to-charge ratio (m/z) ratios [20]. Briefly, its principle is based on ionizing atoms, molecules or clusters from a sample, separating them according to their m/z ratio, and subsequently detecting them and transforming them into mass spectra [21,22]. Ever since the use of mass spectrometry had massively increased, namely by hyphenating mass spectrometer with other separation techniques, at first to gas chromatographs, to analyze volatile organic compounds, and more recently to liquid chromatographs or capillary electrophoresis, to analyze nonvolatile organic compounds. John Fenn endorsed further developments by applying ESI-MS to study large biomolecules and was awarded the Nobel Prize of Chemistry in 2002 for his developments [20,23].

Mass spectrometry coupled to liquid chromatography is nowadays a very important technique. It is worth investing in development of this method, as its properties are highly

remarkable. Some of them are the following:

- 1) It is a very sensitive and highly selective analytical method.
- 2) Allows separation of substances, its quantification and identification via standards and/or measured spectra.
- 3) Provides reproducible information about molecular mass and structure of the analyzed substances.
- 4) Measures concentrations up to nM or even to pM for some compounds [24].

A mass spectrometer usually consists of three major parts: ion source, mass analyzer and detector. Pumps and a computer are common components of this apparatus. Mass analyzers and detectors operate at low pressure, thus an efficient vacuum pumping system is required. A computer stores acquired data and with proper software the data can be processed [25,26].

2.3.1.1 Ion sources

The region in which the analyte molecules are ionized and transformed into the gas phase ions is called the ion source. Ion sources can be classified according to the energy applied to the molecule or according to the pressure under which they operate. The more energy is put onto the molecule, the higher fragmentation results. An example of this high energy fragmentation process is electron impact (EI) ionization [25,26], where the molecules are fragmented and ionized using 70 eV energy. The EI ionization as well as chemical ionization (CI) operates at low pressures ($\sim 10^{-5}$ mbar) [27]. The most common sources operated at atmospheric pressure are electrospray ionization (ESI), atmospheric pressure chemical ionization (APCI) and atmospheric pressure photoionization (APPI).

2.3.1.2 Mass analyzers

A mass analyzer is a device that allows species (e.g. atoms, molecules or clusters) to be separated according to their mass-to-charge ratio by applying electromagnetic forces [21]. Ion separation according to their m/z ratio can be achieved by various physical principles:

- 1) Curvature of the ions flight path either in magnetic or electric field – magnetic analyzers.
- 2) Ions in quadrupole (Q) and quadrupole ion trap (QIT) are separated due to the oscillations in an electric field as a result of direct current (DC) and high frequency (RF – radio frequency) alternating current combinations.
- 3) Different times of the ions flight (time of flight analyzers – TOF)

4) Various energy absorptions during cycloid movements of ions in combined electric and magnetic field (ion cyclotron resonance – ICR) [28].

2.3.1.3 Detector - ion analysis

The detector used is a conversion dynode based system, which makes the highly sensitive detection of both negative and positive ions possible. The detector also has an ion lens, which directs the ions into the detector [27].

2.3.1.4 Tandem mass spectrometry

Tandem mass spectrometry (MS/MS) is a mass spectral technique where controlled ion fragmentation is induced. The new product masses may be either lower or greater than the mother mass as the ion can either be decomposed or may collide with a “reactive” neutral species and thus the heavier product is formed. MS/MS aids greatly in getting information about the structure of compounds [29]. The device we were working with has the capacity to fragment the ions up to the MS^{11} . This means that after fragmentation a daughter ion might be isolated and fragmented again (see Fig. 8). The process can be sequentially repeated for 11 times. The fragmentation of the isolated ions takes place by collision with helium atoms present in the ion trap at pressures of the order of 10^{-5} mbar.

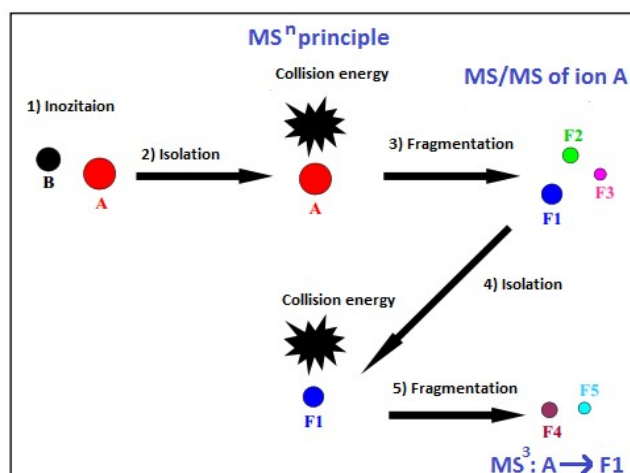


Figure 8 Principle of tandem mass spectrometry.

2.3.2 Chromatographic methods

Chromatographic methods such as gas chromatography (GC) and high performance liquid chromatography are frequently used in analysis of polar pesticides in the

environment. Neither one represents big advantage over the other in analysis of these compounds [30]. HPLC, however, is more suitable technique for analysis of thermally labile and polar compounds, such as carbamates and their degradation products [45].

2.3.2.1 High performance liquid chromatography

HPLC is a method in which individual substances are separated from a mixture based on their distribution between mobile and stationary phases. Nowadays, we can distinguish between two basic modes, normal (NP-HPLC) and reverse (RP-HPLC) phase mode, and hydrophilic interaction chromatography (HILIC). NP-HPLC is the oldest used chromatographic mode where polar phase, such as silica gel or alumina, are used as stationary phase. Hydrocarbons, frequently hexane or heptane, represent the main components of a mobile phase in this system. Polarity of the mobile phase can be increased by addition of alcohols. In RP-HPLC, the distribution of individual components occurs within nonpolar stationary phase, such as silica gel modified with apolar groups, e.g. octane or octadecyl phase, and polar mobile phase, e.g. methanol, acetone, buffers or mixtures of them [31,32,33]. HILIC is a technique becoming still more popular where a polar stationary phase attracts and is enriched by the more polar part of the eluent and acts as the retentive element, while the eluent at the same time offers reasonable solvent properties to allow a fast and linear distribution between the two phases [34]. Currently, RP-HPLC is the most frequently used technique due to the possibility of analyzing wide range of analytes, including those that are impossible to be analyzed in GC. In general In HPLC, it is possible to affect the separation not only by selecting a proper stationary phase but also by altering the composition of mobile phase. In RP-HPLC, this can be done by changing the pH, concentration or/and type of the used buffer or organic solvents. Concerning the stationary phase in RP-HPLC, the longer the modifying alkyl chain, the higher is retention of more nonpolar compounds. Concerning the mobile phase, the increase of retention can be achieved at higher buffer content. Higher retention can be accompanied by enhanced selectivity [32,33,35].

2.3.2.1.1 HPLC detectors

Detectors for HPLC can be categorized into three different groups: universal, selective, and specific [36]. The ideal HPLC detector should meet certain characteristics such as high selectivity and low level of noise; good stability and reproducibility; response should be immediate, should have large linear dynamic range, and should be insensitive to the

changes of pressure and temperature. The most common detectors are: spectrophotometric detector, fluorescence detector, and mass spectrometer [35].

Spectrophotometric detectors are the most frequently used ones in which the absorbance of substances in UV/VIS region of spectra is observed. They may be included into universal detectors. Moreover, they meet quite wide linear dynamic range and low limits of detection [37]. Typically, the simple ones use one or two variable wavelengths. Diode array detection (DAD), however, currently becomes more popular. The entire spectrum can be monitored in real time without interrupting the separation and causing the decrease in sensitivity [38].

2.3.2.1.2 Processing of measured data

Retention factor k is suitable to compare retention of the analytes and characterizes the degree of interaction with the stationary phase. Those values are obtained by using the following equation:

$$k = (t_R - t_M) / t_M \quad (4)$$

where t_R is the retention time and t_M is the dead time of the column.

t_R - the total time the analyte remains in the separation column

t_M - time of the column or time of the components in the sample that is not held in the column and moves with the same speed as the mobile phase

Distribution of two adjacent peaks can be perfect or peak can overlap. Resolution characterizes the degree of mutual overlap of the two neighboring peaks and is defined as follows:

$$R_{1,2} = 2 \times (t_{R,2} - t_{R,1}) / (w_1 + w_2) \quad (5)$$

where $t_{R,1}$ and $t_{R,2}$ are the retention times of the eluting analytes and the w_1 and w_2 are the peak widths at the base. If the value of $R_{1,2}$ is higher or equal to 1.5, the peaks are separated on the baseline.

Separation factor $\alpha_{1,2}$ characterizes the selectivity of the chromatographic system to separated substances. It is the ratio between the two retention factors of analytes and is described by following equation:

$$\alpha_{1,2} = k_2 / k_1 \quad (6)$$

where k_2 is the retention factor of later eluting analyte and k_1 is the factor of earlier eluting analyte. If $\alpha_{1,2} = 1$, no mutual separation of the analytes occurs [31,35].

2.4 Studied pesticides

In this work we chose to study the formation of inclusion complexes of naphthyl (1-naphthylacetamide, 1-naphthylacetic acid) and naphthoxy (carbaryl, napropamide) pesticides with cucurbiturils in aqueous solution. Molecular structures are shown in Fig. 9.

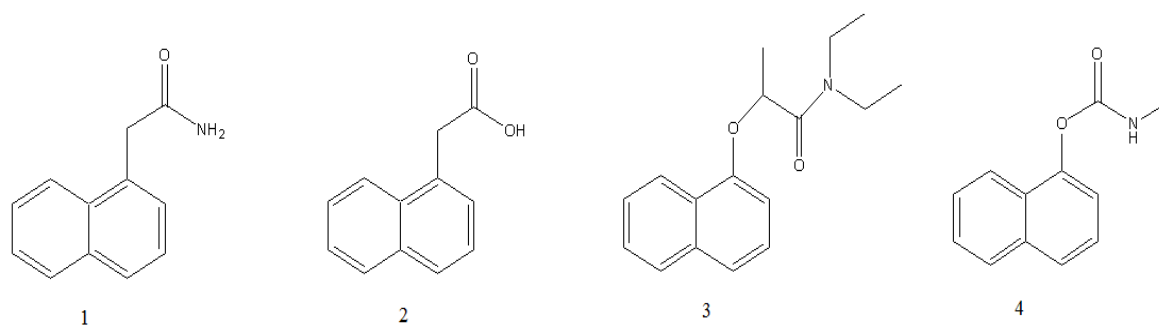


Figure 9 Molecular structures of 1) 1-naphthylacetamide, 2) 1-naphthylacetic acid, 3) napropamide, and 4) carbaryl.

Pesticides are irreplaceable regulators of plant diseases and weeds in modern agriculture. Utilization of pesticides guarantees stable production and quality of crops for constantly growing population. Since many bioactive ingredients are implemented into pesticides, some of them are persistent in soils for many years [39]. Also, their excessive and indiscriminate use can lead to their bioaccumulation in crops, other organisms, and water sources which can consequently cause secondary contaminations through the food chain [39,40]. People have already become more aware of their consequences upon environment, even if used at trace levels, due to the toxicity of these chemicals [40].

Many instrumental methods, among them chromatographic or spectroscopic with high sensitivity and accuracy, have been applied to identify and quantify pesticides [41]. Pesticides that are thermally unstable and thus are not suitable for gas chromatography/mass spectrometry can be monitored by liquid chromatography with tandem mass spectrometry. Electrospray ionization (ESI) and atmospheric pressure chemical ionization (APCI) are most frequently used. Pesticide analysis showed that ESI interface was on average 20 times more sensitive in comparison with APCI interface [42].

These conventional techniques, however, became unsuitable as the need for quick and continuous analysis of large number of samples grew and the pre-treatment procedures are quite time-consuming and expensive. Thus simple and cheaper immunochemical technology was first applied in clinical analysis and subsequently in environmental monitoring of pollutants. Immunoassay methods are considered complementary to liquid and gas chromatography, because they exhibit low detection limits and high selectivity with reduced sample preparation [43].

Carbaryl (Carb) belongs to significant group of pesticides called N-methylcarbamates. They have been first synthesized and commercially introduced in 1950s. Carbamates started to be used as a reimbursement of the organochlorine compounds. They are highly effective as insecticides, herbicides, fungicides, nematocides, acaricides, molluscocides, or sprout inhibitors due to their relatively low mammalian toxicities in many cases, and their low bioaccumulation potentials [44,45]. In addition, carbamates are extensively used in agricultural and forestry industries as acetylcholinesterase-inhibiting insecticides since they have relatively low persistency in the environment compared to organochlorine pesticides [46]. As they inhibit acetyl-cholinesterase, many of them show high acute toxicity and are assumed to be mutagenic, carcinogenic and endocrine disruptors. Growing use of Carb represents quite a risk to aquatic systems and, in relation to this fact, becomes a potential hazard to human health. Thus, the European Union (EU) permits a maximum concentration of $0.1 \text{ ng}\cdot\text{mL}^{-1}$ of each individual pesticide and $0.5 \text{ ng}\cdot\text{mL}^{-1}$ of total in drinking water [47].

Napropamide (NAP) is an amide group of herbicide [48] to prevent the growth of broadleaf weeds and monocotyledon grasses in many agricultural cultivations, such as tea, ground nut, citrus, tobacco, and tomatoes [39,49]. In general, herbicides have become beneficial throughout the whole agriculture. They, however, also can have detrimental effect on environment. Herbicides are one of the most frequent organic pollutants on farmland and thus many questions have risen concerning human health as they mostly contaminate crops and groundwater [50]. Many studies have reported the toxicity of napropamide displaying that inhalation, contact with eyes, skin and clothing should be avoided. It is a polar herbicide, slightly soluble in water and, moreover, its long half-life is approximately 70 days so the residues in soils may have strong affect on the growth of crops. Additionally, it has been estimated that only 0.1 % of herbicides applied to crops reach their target and thus, it can easily contaminate wastewater, rivers and river sediments (due to its fair adsorption/desorption) [48,49,50,51]. In recent literature, many methods for separation and determination of napropamide have been proposed, such as high

performance liquid chromatography (HPLC), supercritical fluid chromatography (SFC), gas chromatography-mass spectrometry (GC-MS), liquid chromatography-mass spectrometry (LC-MS), enzyme-linked immunoassay (ELISA), or spectrofluorimetry [51,52]. Photochemical transformation is an important dissipation way of pesticides in natural conditions [53]. Even though the first-order half-lives for photodegradation have been previously reported, the degradation products were first identified by Tseng *et al.* [54]. It is, however, very difficult to determine how the xenobiotic specific molecule photochemically degrades in nature. Fortunately, examination of the photochemistry of one chromophoric group common to studied pesticides in solution or on the surfaces can serve as a model for the family. The chromophore of napropamide is the naphthyl group. It undergoes photo-Claisen re-arrangements in aqueous media (see Fig. 10) [53].

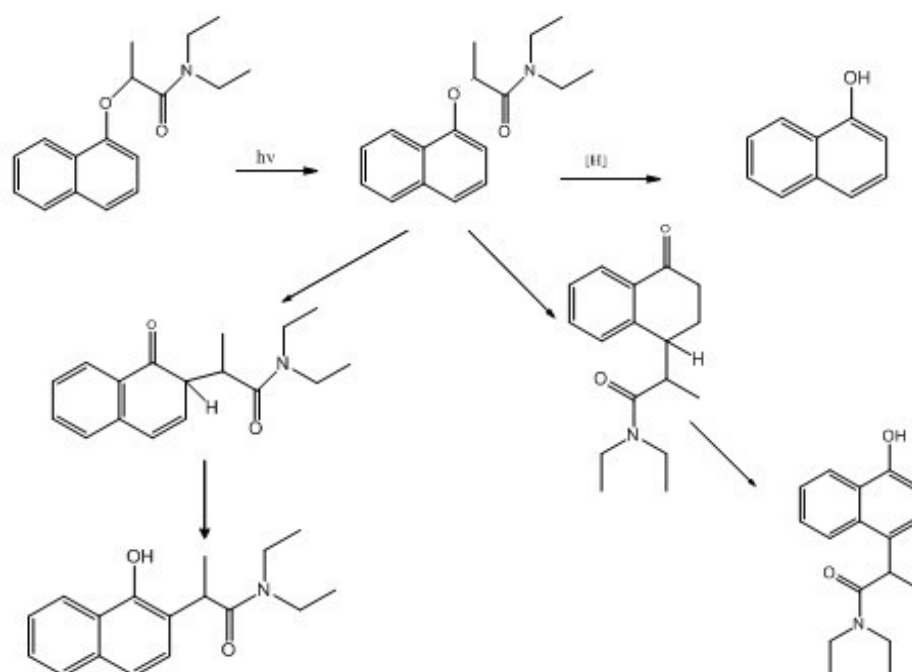


Figure 10 Photo-Claisen reactions of napropamide.

Both 1-naphthylacetamide (NAAm) and 1-naphthylacetic acid (NAA) fall into the same category of pesticides, particularly phytohormones [55]. Most of the published researches do not include simultaneous determination of these compounds, which is probably due to hydrolysis of NAAm into NAA [56]. They have been widely used as growth regulators to prevent the premature fall of fruits. They are also used, combined with other chemicals, as a thinning fruit agent by spraying [57]. There were several unsuccessful attempts to replace

these regulators with Sevin (N-methyl-1-naphthylcarbamate), since the carbamate is extremely toxic to honeybees. Despite the fact that NAAM causes less damage by burning to the leaves than NAA, it is less frequently used [58]. Similarly to other studied pesticides, the most frequent methods used to identify and determine all residues include biological assays, immunological essays and physical detection procedures [55]. Ever since Sigrist *et al.* [58] introduced first fluorimetric method for simultaneous determination of NAAM and NAA, the field of suitable instrumental techniques have widened, e.g., spectrophotometric, spectrofluorimetric and chromatographic techniques, and/or room temperature phosphorescence (RTP) [57,59].

3 Objectives

The formation of inclusion complexes of naphthyl (1-naphthylacetamide, 1-naphthylacetic acid) and naphthoxy (carbaryl, napropamide) pesticides into cucurbiturils and cyclodextrins was to be studied in aqueous solution. The formation of complexes was to be followed by UV-Vis absorption, and electrospray ionization mass spectrometry. The photo-transformation of the above mentioned pesticides was to be studied in aqueous solutions, with and without CBs and CDs. We expect to detect the formation of the complexes and obtain their stoichiometry. The main photo-transformation products were to be identified using chromatography and mass spectrometry techniques.

The aims of this work can be summarized in the following points:

- 1) Identification and description of fundamentals of supramolecular chemistry and photochemistry.
- 2) Description of the behavior of cucurbiturils and cyclodextrins as nano-containers for organic molecules and prediction of the formation of host-guest complexes.
- 3) Optimization of ESI-MS conditions to obtain structural information on host-guest complexes of CBs with pesticides.
- 4) Optimization of spectrophotometric and HPLC conditions to obtain knowledge on the effect of complexation on degradation rate of pesticides exposed to UV light in presence/absence of CBs or CDs.

4 Experimental part

4.1 Solvents

Table 4 summarizes used solvents during the work

Table 4 List of solvents used

Name of the substance	Manufacturer	Purity
Acetonitrile	Sigma-Aldrich, Steinheim, Germany	≥ 99.9 %
Methanol for HPLC (Chromasolv ®)	Sigma-Aldrich, Steinheim, Germany	≥ 99.8 %
Distilled water	Watrex, Prague, Czech Republic	

4.2 Organic compounds

- 1-naphthylacetic acid (Riedel-de Haën, Hanover, Germany, purity 94.3 %)
- 1-naphthylacetic acid (Sigma-Aldrich, Steinheim, Germany)
- 1-naphthylacetamide (Riedel-de Haën, Hanover, Germany, purity 99.3 %)
- 1-naphthylacetamide (Fluka, Steinheim, Germany purity 99.0 %)
- Carbaryl (Riedel-de Haën, Hanover, Germany, purity 99.8 %)
- Napropamide (Chem. Service, West Chester, USA, purity 99.0 %)
- Cucurbit[7]uril (Sigma-Aldrich, Steinheim, Germany)
- Cucurbit[7]uril (Strem Chemicals, Newburyport, USA purity ≥ 99%)
- Cucurbit[8]uril, generous gift by Prof. Ramamurthy, from Miami University
- β-cyclodextrin (Sigma-Aldrich, Steinheim, Germany, purity ≥ 98.0 %)

4.3 Equipment

Direct injections were made onto a mass spectrometer Bruker Daltonics (Coventry, UK) HCTultra, which was equipped with syringe pump Kd Scientific, electrospray ionization ion source Agilent (Santa Clara, USA) and quadrupole high capacity ion trap all from Bruker Daltonics (Coventry, UK).

Spectra were collected using esquireControl version 6.1, software provided by Bruker

Daltonics (Coventry, UK), and evaluated using DataAnalysis, version 3.4, also by Bruker Daltonics (Coventry, UK).

Analytes were also measured on spectrophotometer Shimadzu (Kyoto, Japan) UV-2400PC Series. The data collection and evaluation was done by UVProbe version 2.35.

Chromatograms were obtained on the liquid chromatograph Agilent Technologies (Santa Clara, USA) 1200 Series, which was equipped with degasser, quaternary pump, autosampler, column compartment and diode array detector (DAD). The polymeric octadecyl reverse phase column used for the chromatographic separations was Hamilton (Reno, USA) PRP-1 with following properties: length 15 cm, diameter 2.1 mm, and particle diameter 5 μm . LC was hyphenated with mass spectrometer Bruker Daltonics (Coventry, UK) HCTultra. Data collection was done using Agilent (Santa Clara, USA) ChemStation for LC 3D systems, version Rev.B.01.03 (204). Evaluation of the results was done using Bruker Daltonics (Coventry, UK) DataAnalysis, version 3.4.

Measurement was also performed on HPLC equipment composed of the pump Delta Chrom SDS 030 (Watrex, Prague, Czech Republic), dispensing valve with 20 μl loop, dual channel detector UV/VIS Spectra 100. The column Agilent (Santa Clara, USA) Zorbax Eclipse XDB-C18 with octadecyl phase had following dimensions: particle size 5 μm , diameter 4.6 mm, and length 15 cm. Consequently, the data were collected and evaluated by Clarity version 2.1.0.15 (DataApex, Prague, Czech Republic).

Pipettes, Biohit, Helsinki, Finland.

The mobile phases were sonicated in ultrasonic bath P-Lab (ELMA, Germany) LC 30 before use

Balance Mettler AE 240, Greifensee, Switzerland.

4.4 Sample preparation

Aqueous stock solutions of 1-naphthylacetic acid, 1-naphthylacetamide, carbaryl and napropamide were prepared in the concentration of 1 mg/l, followed by filtering in order to remove any possible particles inside the solutions. Consequently, these concentrations were diluted to desired concentrations.

Concerning preparation of the host-guest complexes, we had to consider the saturation point of CB[8] as it is close to 100 μM . Nevertheless, all complexes were prepared as follows: 50 μM of CBn ($n = 7$ and 8) and 25 μM of each pesticide and *vice versa*.

4.5 Sample irradiation

Samples irradiation was performed in quartz cells, using low pressure mercury lamp under the power of 16 W and maximum emission at 254 nm, placed in a distance of 1 cm.

Irradiation times of each pesticide differed as these particular analytes degrade after different periods of exposure to UV light.

4.6 Measurement conditions

4.6.1 Mass spectrometer

The infusion was carried out under the following conditions: the infusion flow was set to 240 μ l/hour, capillary was set to 4000 V, nebulizer to 20 psi, drying gas flow rate of 6 l/min and heated to 300°C, skimmer and capillary exit were set to power of 15 V and 66.7 V, respectively. The mass spectrometer was run in positive ion mode and the m/z ranged between 50 and 3000. Measurements were done in Portugal.

4.6.2 Liquid chromatograph

The LC-MS measurements were carried out in Portugal under the following conditions: the column flow was set to 0.40 ml/min, the maximum pressure of the pump was set to 400 bars, the diode array detector ranged from 190 nm to 400 nm and the thermostat was set to 25°C. Injection volume was 5 μ l. Table 5 presents the gradient elution.

Table 5 Gradient elution

Time [min]	Acetonitrile [%]	Flow rate [ml/min]
0,00	20,0	0,40
20,00	100,0	0,40
24,00	100,0	0,40
25,00	20,0	0,40
30,00	20,0	0,40

The mass spectrometer conditions used under LC-MS were similar to those used under infusion but the nebulizer was set to 20 psi and the drying gas was flowing at the rate of 10 l/min.

The conditions under which the experiments were carried out in Czech Republic on the liquid chromatograph Delta Chrom SDS 030 were following: the column flow was set to 1 ml/min, the pressure at the given flow rate was approximately 80 bars, injection volume was 25 μ l, and the detector was set to 280 nm. Optimized mobile phases of acetonitrile/H₂O for NAP, CARB, NAAM, and NAAc were used in the following ratios (v/v): 50/50, 30/70, 25/75, and 35/65, respectively. In order to improve retention of NAAc, the mobile phase was acidified with formic acid to the pH 3 (pH of the aqueous part of the mobile phase). All injections were repeated three times.

4.6.3 Spectrophotometer

The measurement conditions were as follows: wavelength ranged between 200 nm and 600 nm, sampling interval was 0.5. Concerning the absorbance, the slit width was set to 1.0 nm and the light source wavelength was changed at 325 nm. The absorbance values were, for further evaluation, collected at the wavelength of absorption maxima (minima). The measurements were carried out in Czech Republic.

5 Results and discussion

5.1 ESI-MS

We started by injecting CB7 and CB8 in aqueous solution without any guest molecules. For CB7 two peaks were readily seen at m/z 582 and 1163 (see Fig. 11).

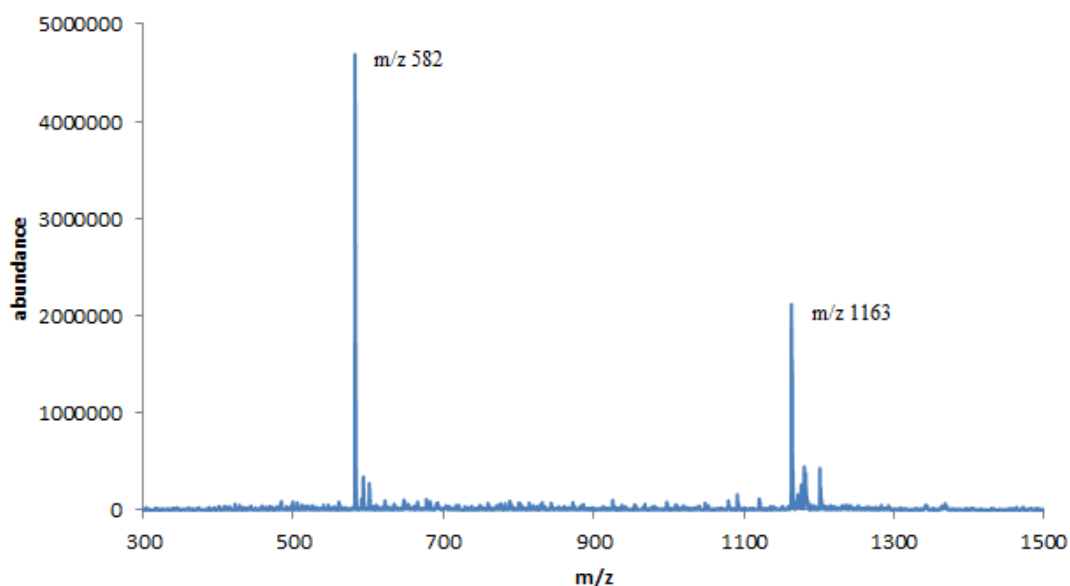


Figure 11 ESI-MS spectrum of CB[7] in aqueous solution. Conditions: $c(\text{CB7}) = 100 \mu\text{g/l}$ the infusion flow was set to $240 \mu\text{l/hour}$, capillary was set to 4000 V , nebulizer to 20 psi , drying gas was flowing at the rate of 6 l/min and heated to 300°C , skimmer and capillary exit were set to power of 15 V and 66.7 V , respectively. The mass spectrometer was run in positive ion mode and the m/z ranged between 50 and 3000 .

Detailed analysis of these peaks showed 0.5 and 1.0 isotope spacing of m/z 582 and 1163 , respectively (see Fig. 12).

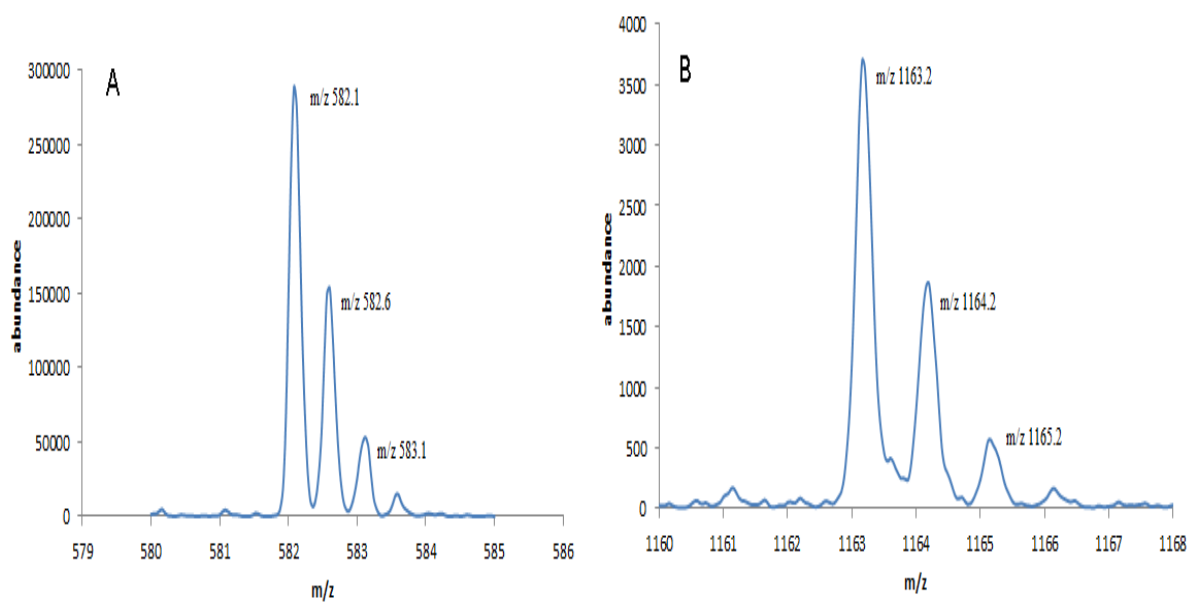


Figure 12 Isotope spacing for A) m/z 582 and B) 1163.

This is consistent with a doubly charged ion for 582 and single charge ion for 1163. The m/z values, together with the charged states, indicate the ions at m/z 582 and 1163 have the structures $[\text{CB7}+2\text{H}]^{2+}$ and $[\text{CB7}+\text{H}]^+$, respectively. When Na^+ is present in solution the doubly charged and single charged signals change to 604 and 1185, respectively, indicating the formation of Na^+ adducts instead of H^+ adducts. The correspondent signals were observed also when K^+ was present. In CBs, they come into the gas phase as H^+ , Na^+ , K^+ or other positive ion adducts, containing one or two of these ions. Aggregation was also observed, particularly in pure water and soft ionization conditions (capillary exit < 150 V). Dimers and trimers were observed under these conditions, as reported previously [15]. These structures come into the gas phase with two, three and sometimes four charges.

Similar behavior was observed for CB8. In this case, the ions were observed at m/z 665 and 1329. The structures were assigned to $[\text{CB8}+2\text{H}]^{2+}$ and $[\text{CB8}+\text{H}]^+$, respectively. Na^+ adducts were also observed changing the two charge state and single charge state to 687 and 1351, respectively. Similarly to CB7 the dimers and trimers aggregates also appeared.

In the presence of the studied guests the mass spectrum changes completely. Fig. 13 shows the mass spectrum of CB8 in the presence of NAAM.

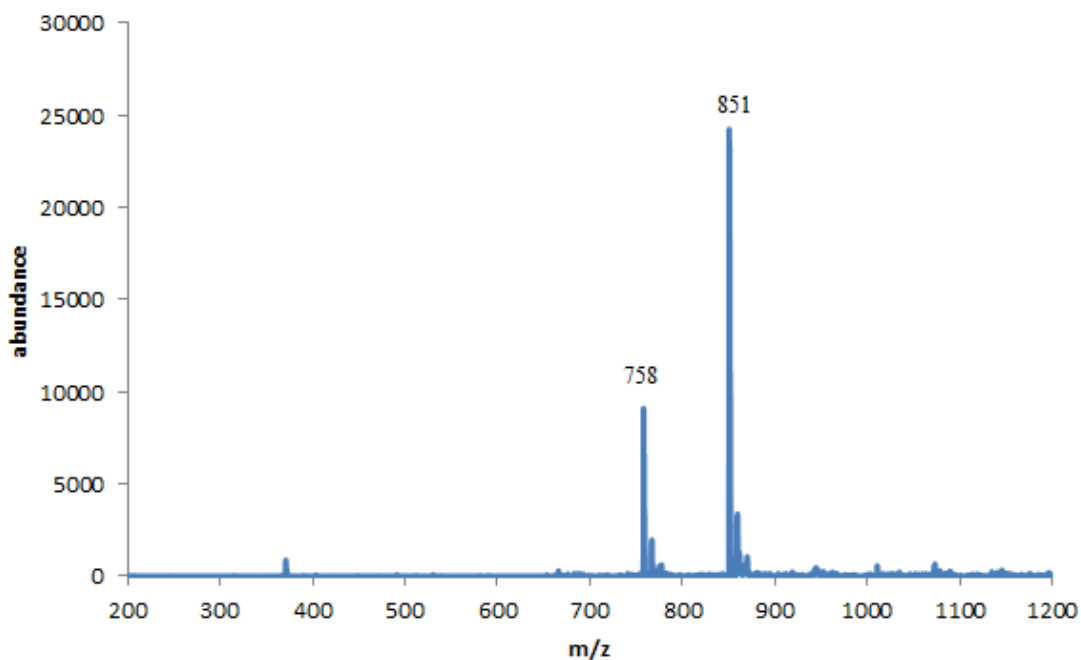


Figure 13 Mass spectrum of NAAM encapsulated to CB8. Conditions: $c(\text{CB8}) = 100 \mu\text{g/l}$. Other conditions as in Fig. 11.

Base peaks at m/z 851 together with a lower intensity one at m/z 758 were observed. The isotope distributions indicated that both peaks have two charges. MS^2 of m/z 851 leads to the formation of 758 and 665, which corresponds to neutral losses of 186 and 2×186 (see Fig. 14).

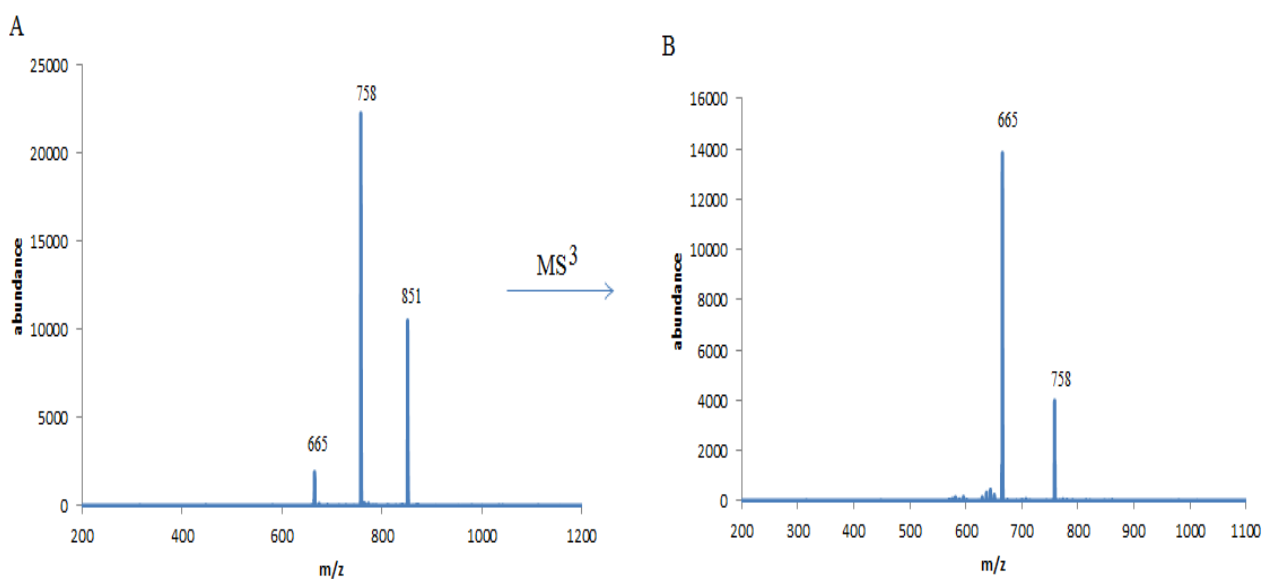


Figure 14 Fragmentation mass spectra A) MS^2 and B) MS^3 of NAAM encapsulated into CB8. Conditions: $c(\text{CB8}) = 100 \mu\text{g/l}$. Other conditions as in Fig. 11.

These values correspond to losses of one and two guest molecules, respectively. We assign therefore the ion at m/z 851 to the 1:2 (host:guest) complex. The fragmentation (MS^3) of m/z 758 leads to 665 (see Fig. 14), causing the loss of 186 Da. The ion at m/z 758 was assigned to the 1:1 (host:guest) complex.

In the presence of CB7, peaks at m/z 786 and 694 were observed. The isotope distribution revealed that both of them are doubly charged. Further fragmentation of m/z 786 gave rise to 582 as well as MS^2 of m/z 694 led to 582. The neutral loss is therefore 2×186 and 186, respectively. The ion at m/z 786 was assigned to 1:2 (host:guest) complex and ion at m/z 694 to 1:1 (host:guest) complex.

ESI-MS clearly shows that CB8 and CB7 form 1:1 and 1:2 complexes with NAAM.

When we introduced NAAC with CB8 present into the system, we were able to see one major ion at m/z 758. The 0.5 isotope spacing indicated that observed ion is doubly charged. Tandem mass spectrometry of m/z 758 led to formation of 665 and 1329. The neutral loss was 185. We could therefore define the structure as 1:1 (host:guest) complex $[CB8 + \text{guest} + 2H]^{2+}$.

Formed 1:1 complexes were also seen in the presence of CB7. After an infusion, the mass spectrometer detected m/z 470 and 694. The 0.3 and 0.5 isotope spacing showed that we dealt with triply and doubly charged ions. MS^2 of m/z 470 led to the formation of m/z 694. MS^3 of this ion gave rise to m/z 582. This corresponds to neutral loss of 185 in both cases. The ion structures were therefore assigned as 1:1 (host:guest) complexes $[CB7 + \text{guest} + H_2O + 3H]^{3+}$ and $[CB7 + \text{guest} + H_2O + Na + 2H]^{2+}$, respectively. We can see that the ion at m/z 694 is consistent with Na^+ adduct.

ESI-MS gives us information that NAAC in the presence of CBs forms 1:1 complexes only.

Direct injections of NAP in the presence of CB8 showed 3 major ions at m/z 810, 937 and 1601. The 0.5 and 1.0 isotope spacing corresponded to doubly charge states of 810 and 937 and singly charge state of 1601. MS/MS of 810 formed ions at m/z 1329 and m/z of NAP 272. We thus assumed the structure of 1:1 complex $[CB8 + NAP + H_2O + 2H]^{2+}$. Fig. 15 represents the fragmentation mass spectrum (MS^2) of CB8 in the presence of NAP.

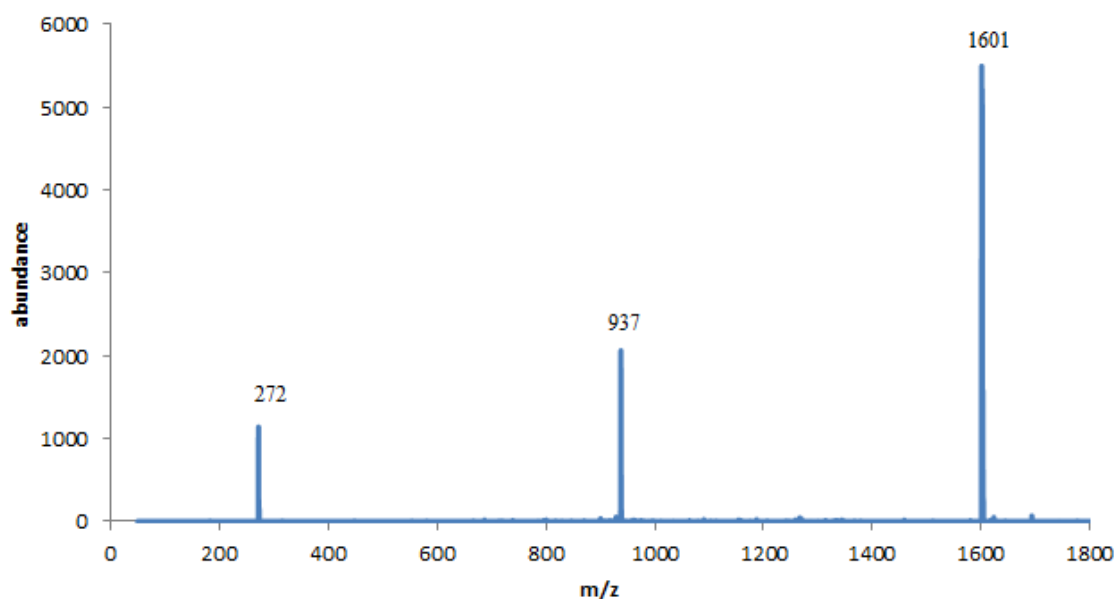


Figure 15 Fragmentation mass spectrum of inclusion complex of NAP with CB8. Conditions: $c(\text{CB7}) = 100 \mu\text{g/l}$ Other conditions as in Fig. 11.

Fragmenting the ion at m/z 937 led to m/z 272 and 1601. MS^3 of ion at m/z 1601 broke it into ions at m/z 272 and 1329. The ion distribution showed that 1601 corresponds to singly charged state. Based on the m/z values, isotope distribution and MS^n we could assign the structure as $[\text{CB8} + 2 \text{ guests} + 2\text{H}]^{2+}$ and $[\text{CB8} + \text{guest} + \text{H}]^+$, respectively.

We observed similar behavior when CB7 was present together with NAP. Base peaks 1435 as well as 853 at lower intensity were observed. Isotope distribution showed singly and doubly charged ions, respectively. Fragmentation of ion at m/z 1435 led to the formation of 1163, the loss of 272 Da. MS^2 of 853 gave rise to 1435 and 272. The ions were, based on the provided information by ESI-MS, assigned to $[\text{CB7} + \text{guest} + \text{H}]^+$ and $[\text{CB7} + 2 \text{ guests} + 2\text{H}]^{2+}$.

Carb in the presence of CB8 gave very good response as we were able to define obtained major ions at m/z 867 and 766. The 0.5 isotope spacing uncovered doubly charged ions. MS/MS of 867 changed the m/z to 766 and 665. MS^3 of 766 released the 665 only. Thus ion at m/z 867 is consistent with the neutral loss of 2×202 and ion at m/z corresponds to the loss of 202. The m/z values, isotope distributions and MS^n indicated that these ions have the structure of $[\text{CB8} + 2 \text{ guests} + 2\text{H}]^{2+}$ and $[\text{CB8} + \text{guest} + 2\text{H}]^{2+}$, respectively.

5.2 LC-MS

We were also interested if the encapsulation changes the photoproduct distribution. Fig. 16 shows an illustrative chromatogram of 1-naphthylacetamide alone and 1-naphthylacetamide included into CB7 after 120 minutes of irradiation.

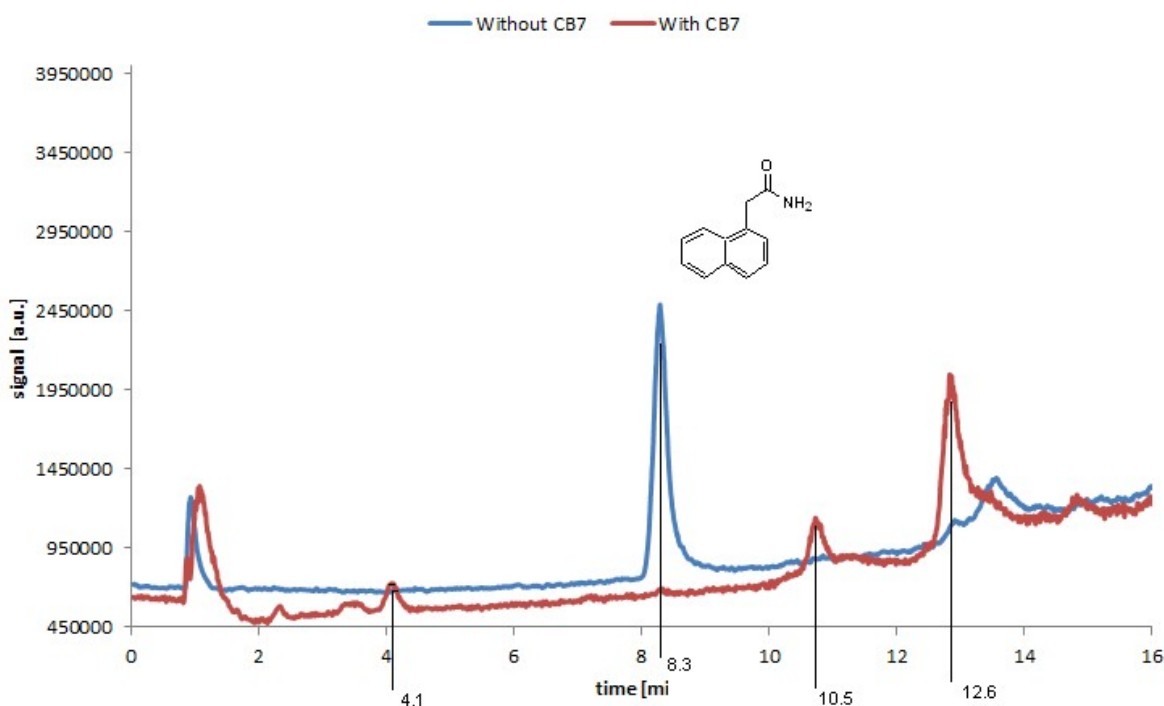


Figure 16 Chromatogram of 1-naphthylacetamide with and without CB7 after 120 minutes of irradiation. Conditions: the column flow was set to 0.400 ml/min, the maximum pressure of the pump was set to 400 bars, the diode array detector ranged from 190 nm to 400 nm and the thermostat was set to 25°C. Injection volume was 5 μ l.

Retention time of non-irradiated NAAM was at 8.3 minutes. New photoproducts of inclusion complex have been formed and released at following times: 4.1 minutes ($m/z = 218$), 10.5 minutes ($m/z = 240$), and 12.6 minutes ($m/z = 329$). Further studies are needed to assign the observed photoproducts.

As da Silva stated, LC trace of napropamide revealed that new photoproducts were formed during the irradiation as *N,N*-diethyl-2-(4-hydroxynaphthalene-1-yl)-propionamide eluted at 10.1 minutes and *N,N*-diethyl-2-(1-hydroxynaphthalene-2-yl)-propionamide was released after 14.3 minutes. Thus, we can say that this particular herbicide undergoes photo-Claisen reaction in aqueous media as well as within cucurbit[8]uril. The C-O bond between the naphthoxy and alkyl group has been cut due to hemolytic scission and

consequently recombined appropriately [53].

The LC trace of Carb did not show any difference in photoproduct distribution in either presence or absence of the CB8.

5.3 Spectrophotometry

5.3.1 Pesticide spectra

Spectrophotometric measurements proved that when both free and included pesticides are exposed to UV light, the analytes degrade progressively in time. Illustrative figures of NAAM and Carb are shown in Fig. 17 and Fig. 18, respectively.

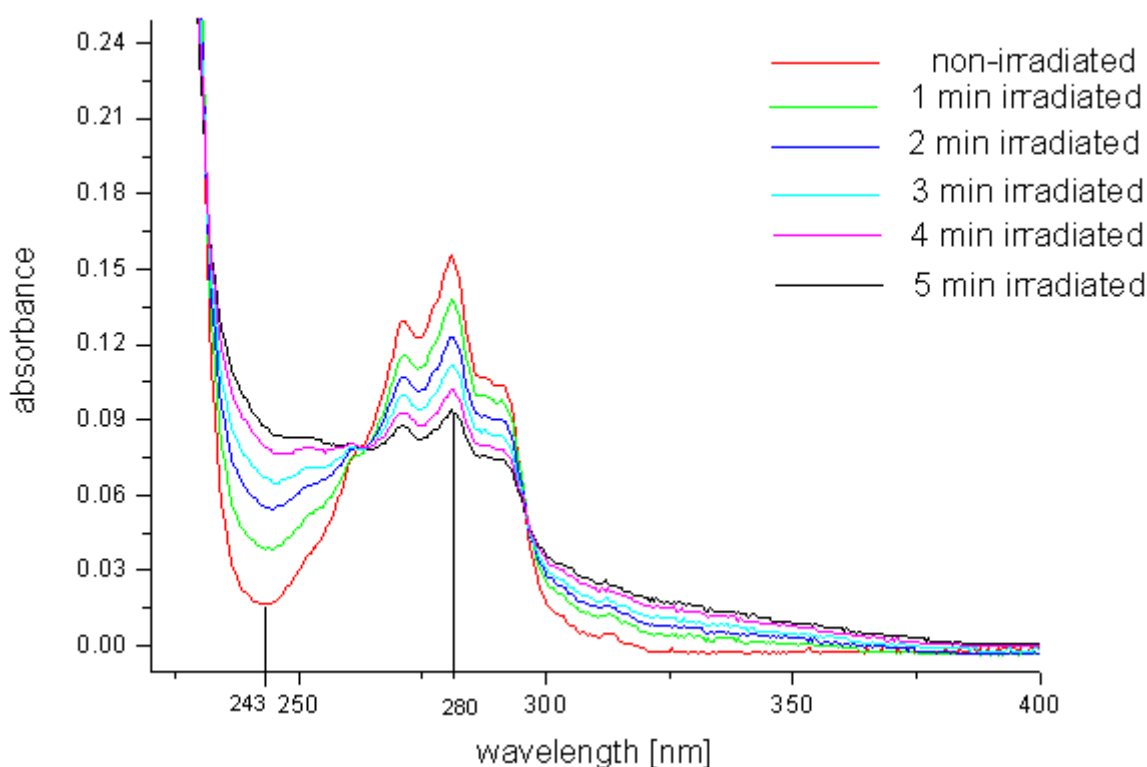


Figure 17 Spectrum of NAAM. Conditions: $c = 100 \mu\text{g/l}$, measured wavelength range from 200 nm to 600 nm (shown just from 220 nm to 40 nm), sampling interval 0.5, the absorbance of slit width 1.0 nm, and the light source wavelength change at 325 nm.

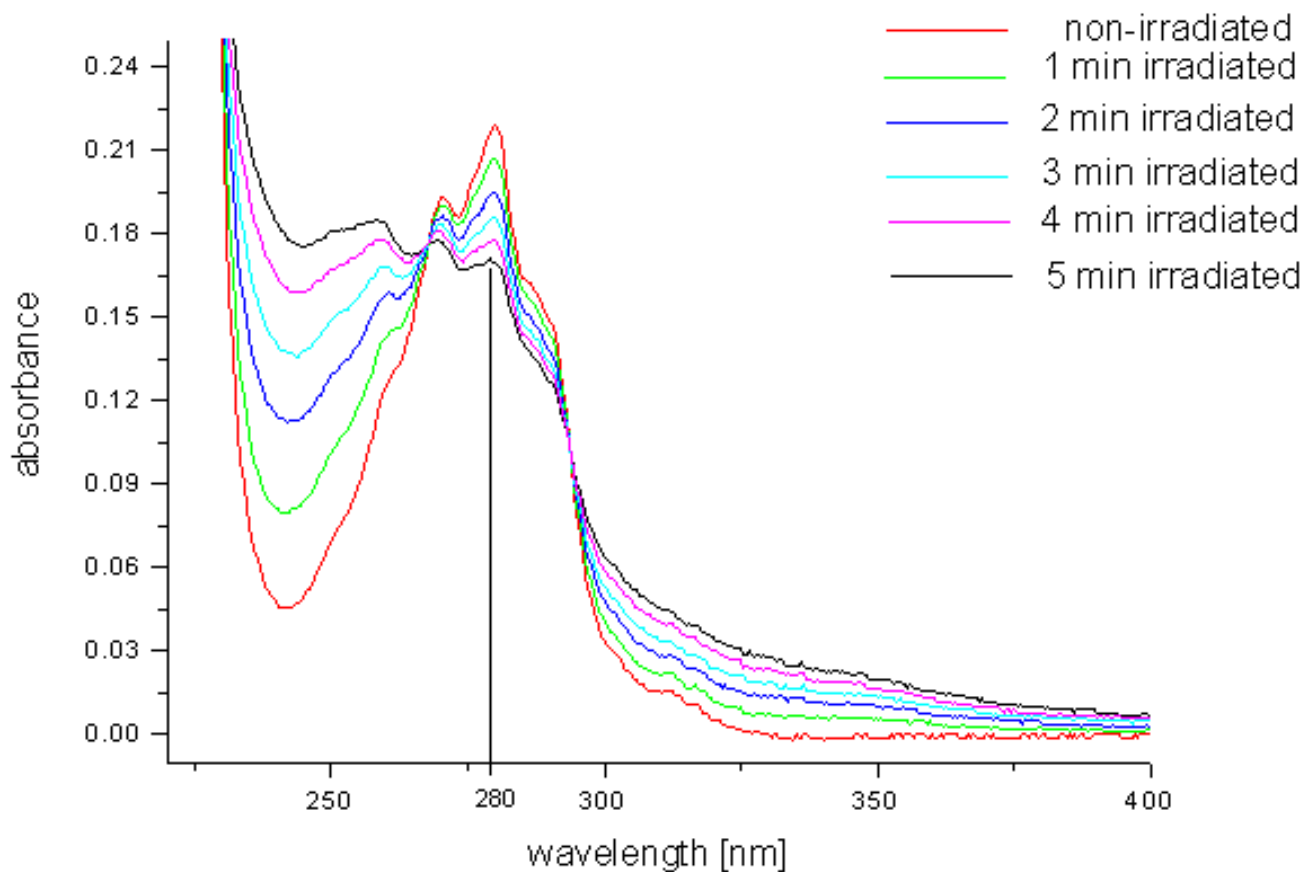


Figure 18 Spectrum of Carb. Conditions: $c = 200 \mu\text{g/l}$, other conditions as in Fig. 17.

The absorption maxima were determined for all pesticides at 280 nm. The spectra confirm photodegradation of the pesticides as the signal decreases.

We could also confirm analogical behavior of encapsulated pesticides within CB and CD, which is shown in illustrative Fig. 19 and Fig. 20, respectively.

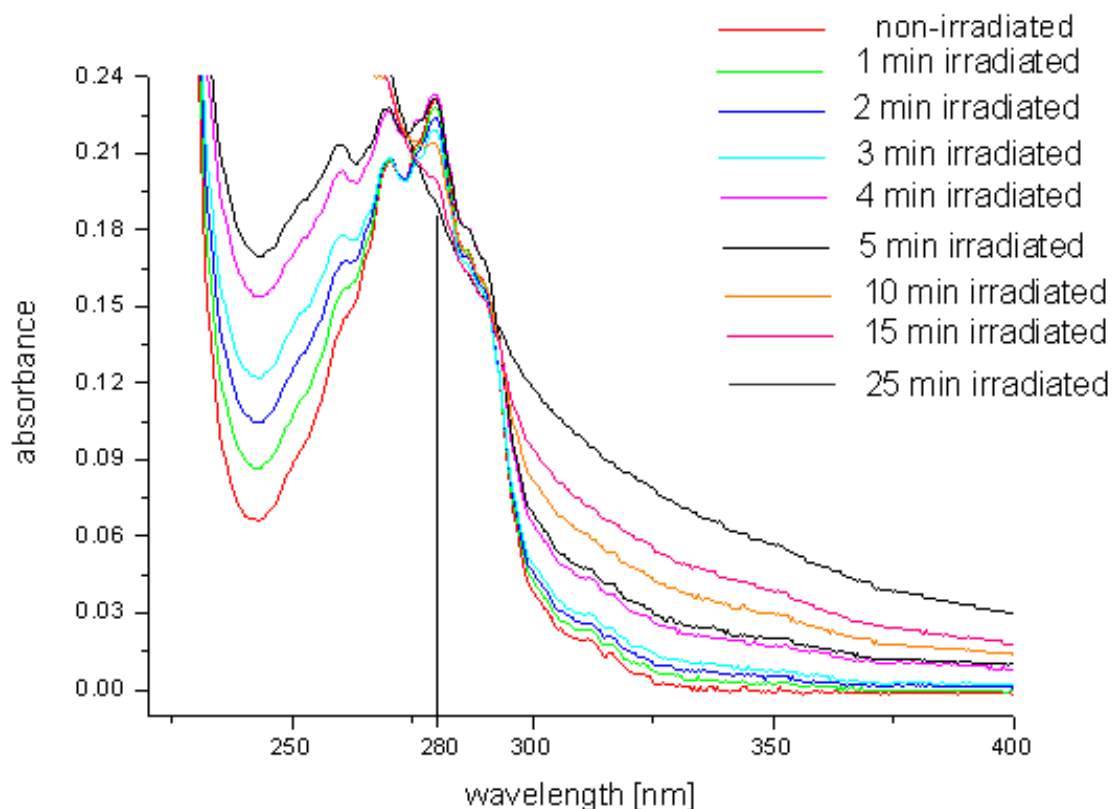


Figure 19 Spectrum of inclusion complex of Carb with CB[7]. Conditions: c [Carb] = 200 $\mu\text{g/l}$, c [CB] = 100 $\mu\text{g/l}$, other conditions as in Fig. 17.

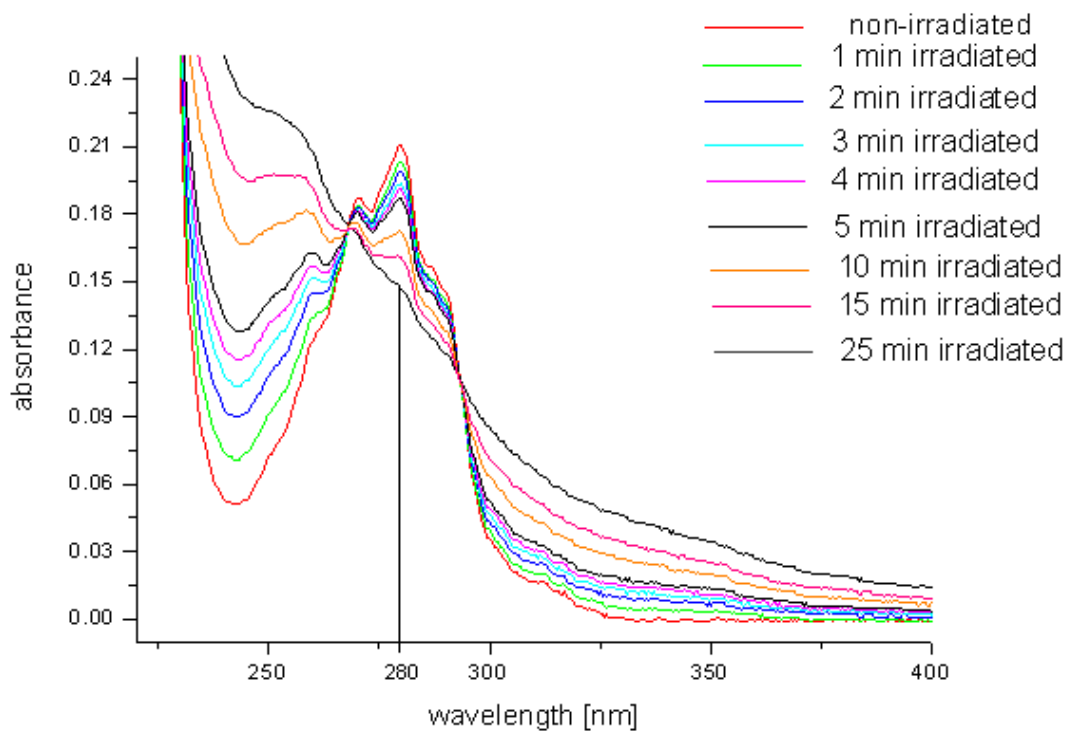


Figure 20 Spectrum of inclusion complex of Carb with β -CB. Conditions: c [Carb] =

200 $\mu\text{g/l}$, $c [\text{CB}] = 100 \mu\text{g/l}$, other conditions as in Fig. 17.

The comparison of spectra of free and included Carb shows significant changes. Thus, we can say that the encapsulation process affects the pesticide decomposition.

Similar results were obtained for the other pesticides.

5.3.2 Rate constants determination

We aimed to obtain the rate constants of decomposition of the pesticides without and with host molecules (CB or CD) in the solution. As our analytes were successively irradiated, the dependences of absorbance on time were plotted followed by fitting by an exponential function. Consequently, the dependences of natural logarithm of absorbance on time were plotted from which the slope value was obtained. The positive value of the slope gave the rate constant value. Absorbance values were subtracted at the wavelength of both the “valley” (minimum) and maximum (latest irradiated spectrum was defined as our baseline) in the spectra (see Fig. 17) and then the obtained values were compared. Given that the obtained values were similar (see Tab. 6) we introduce the rate constants subtracted only from the maximum of the spectra.

The dependence of absorbance on time of Carb is shown in Fig. 21.

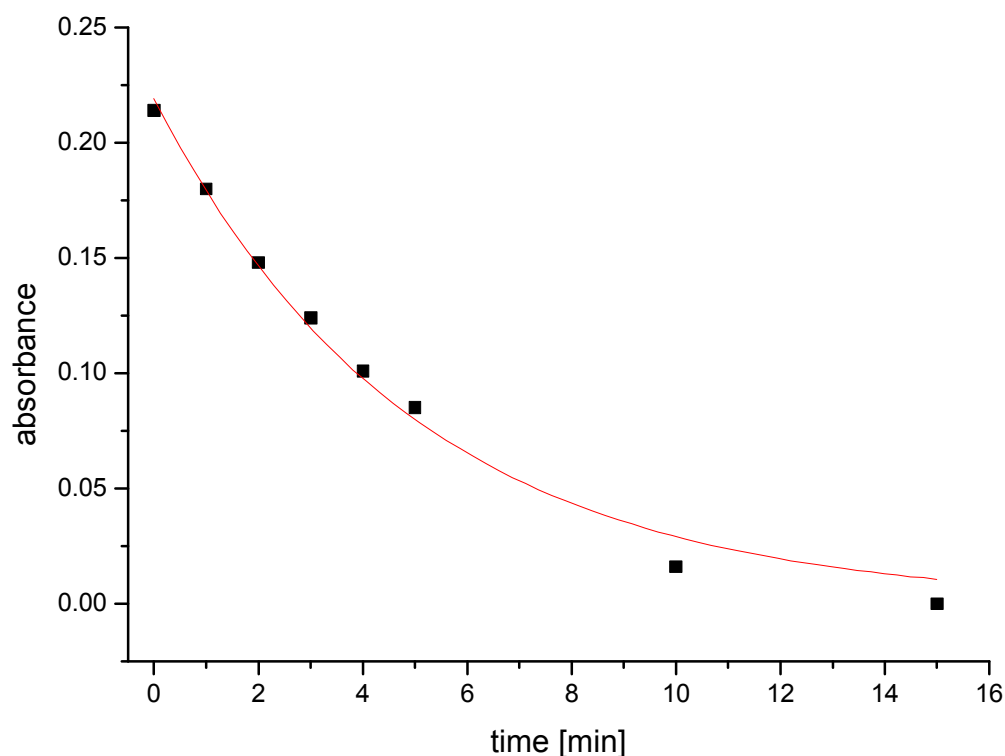


Figure 21 Dependence of absorbance on time of Carb.

The dependence of natural logarithm of absorbance on time of carbaryl can be seen in Fig. 22.

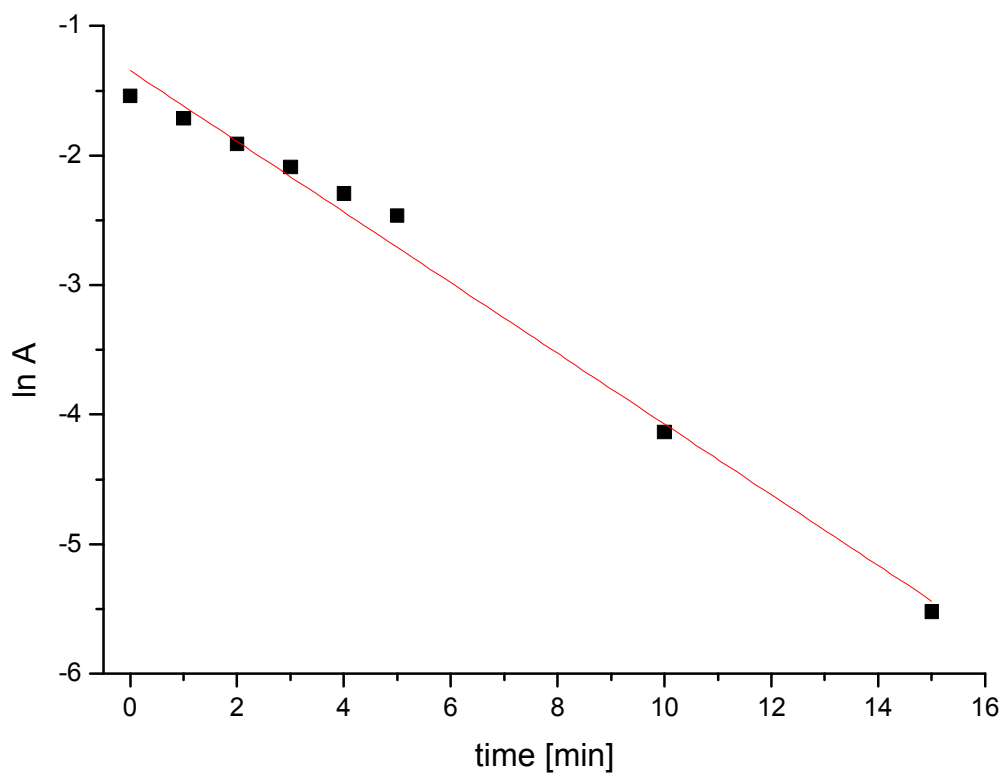


Figure 22 Dependence of natural logarithm of absorbance on time of Carb.

Analogically, both graphs of included carbaryl into CB7 and CD are presented in Fig. 23, Fig. 24, and Fig. 25, Fig. 26, respectively.

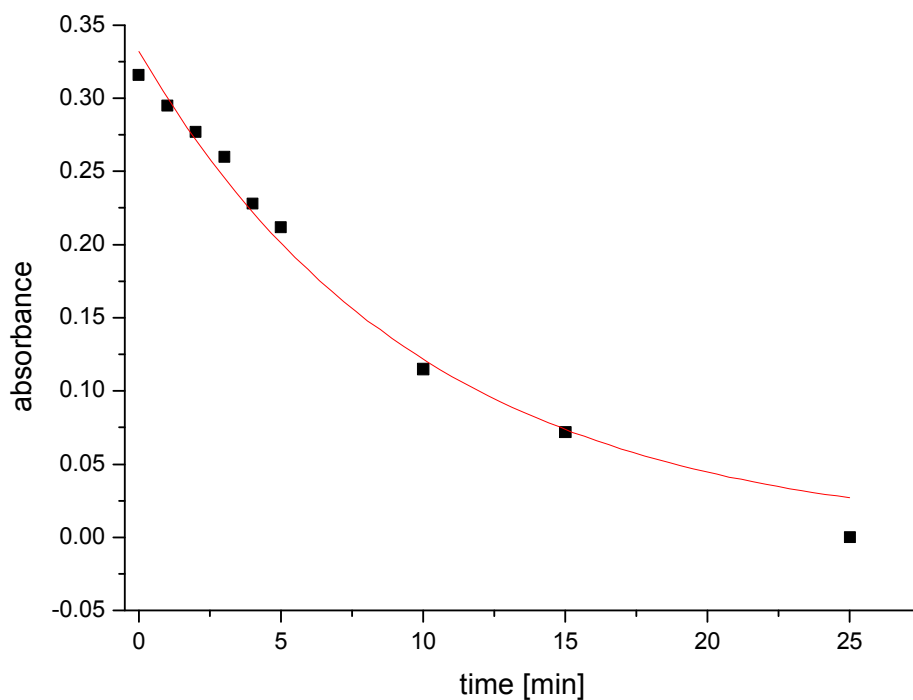


Figure 23 Dependence of absorbance on time of inclusion complex of Carb with CB[7].

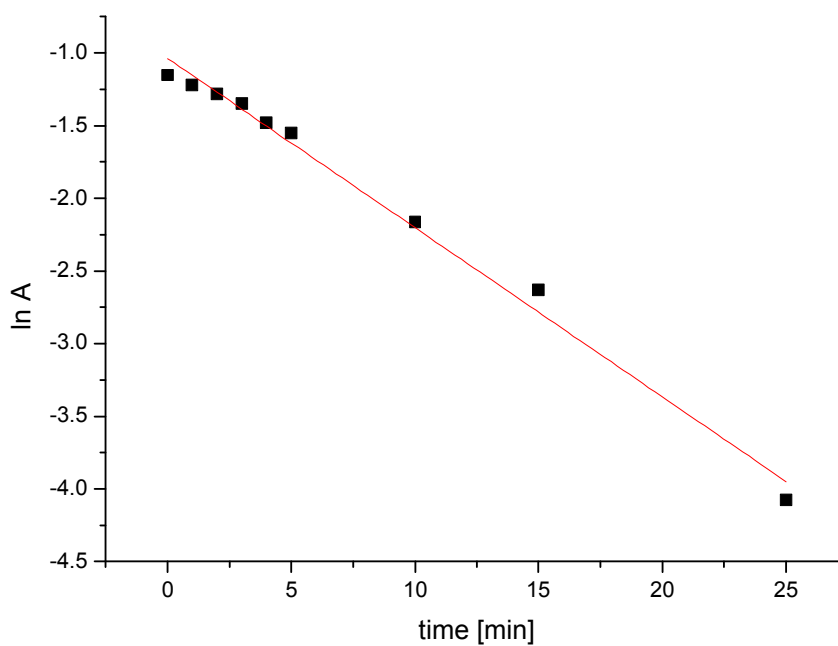


Figure 24 Dependence of natural logarithm of absorbance on time of inclusion complex of Carb with CB[7].

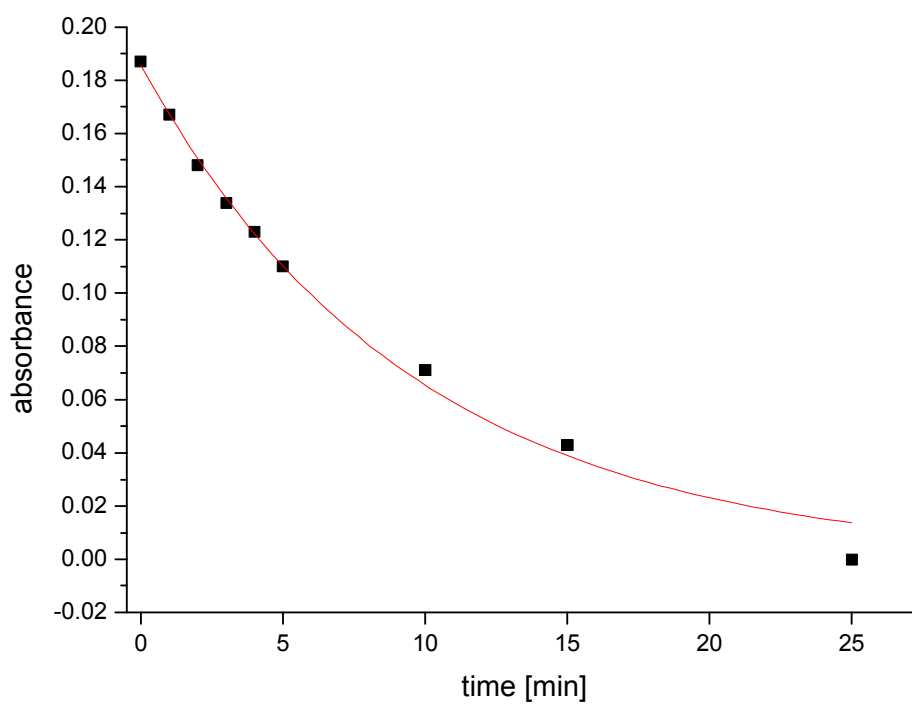


Figure 25 Dependence of absorbance on time of inclusion complex of Carb with β -CD.

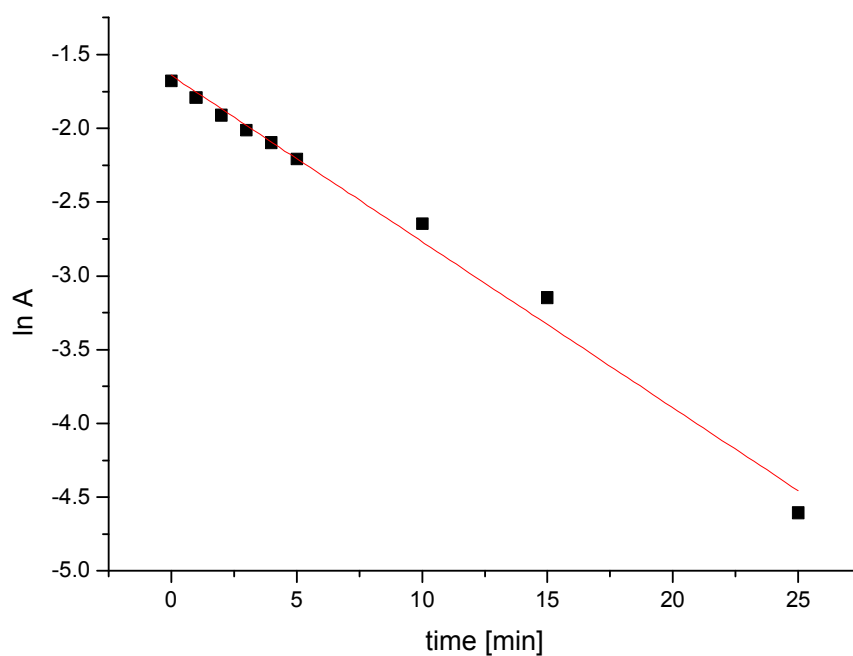


Figure 26 Dependence of natural logarithm of absorbance on time of inclusion complex of Carb with β -CD.

Obtained rate constants are summarized in Tab. 6.

Table 6 Rate constants of pesticides degradation

Pesticide	K_x	R
NAAm maximum	0.286	0.9966
NAAm valley	0.252	0.9944
NAAm@CB7	0.137	0.9863
NAAm@β-CD	0.581	0.9493
NAAc	0.617	0.8516
NAAc@CB7	0.824	0.9867
NAAc@β-CD	0.943	0.9657
Carb	0.273	0.9946
Carb@CB7	0.117	0.9955
Carb@β-CD	0.112	0.9944
NAP	0.689	0.9836
NAP@CB7	0.409	0.9849
NAP@β-CD	0.376	0.9655

The results show somewhat incomparable values. NAAm, considering the degradation rate, falls apart in following order: NAAm@β-CD > NAAm > NAAm@CB7.

This tendency, however, is not maintained for other pesticides. In case of NAAc, fastest degrades NAAc@β-CD, followed by the inclusion complex NAAc@CB7, and the last one is NAAc.

The results for Carb and NAP seem to be logical.

Considering Carb, the degradation trend is exactly the opposite of the NAAc, particularly the first to disintegrate comes Carb, followed by the inclusion complex Carb@CB7, and completed by the Carb@β-CD.

NAP is analogical to its naphthoxy “brother” and degrades exactly in the same order.

Comparing acquired rate constants with stability constants obtained by Magda Örgödvová by capillary electrophoresis measurement [14]. If the pesticide is included into

CD, the slowest photodegradation correlates well with high stability constant obtained for β -CD while the complex with CB could not be even measured.

5.4 HPLC

5.4.1 Pesticide analysis

Chromatographic analysis also proved that the pesticides progressively degrade in time under the UV light and thus verified results obtained by previously applied methods. Illustrative chromatograms of NAP are shown in Fig. 27.

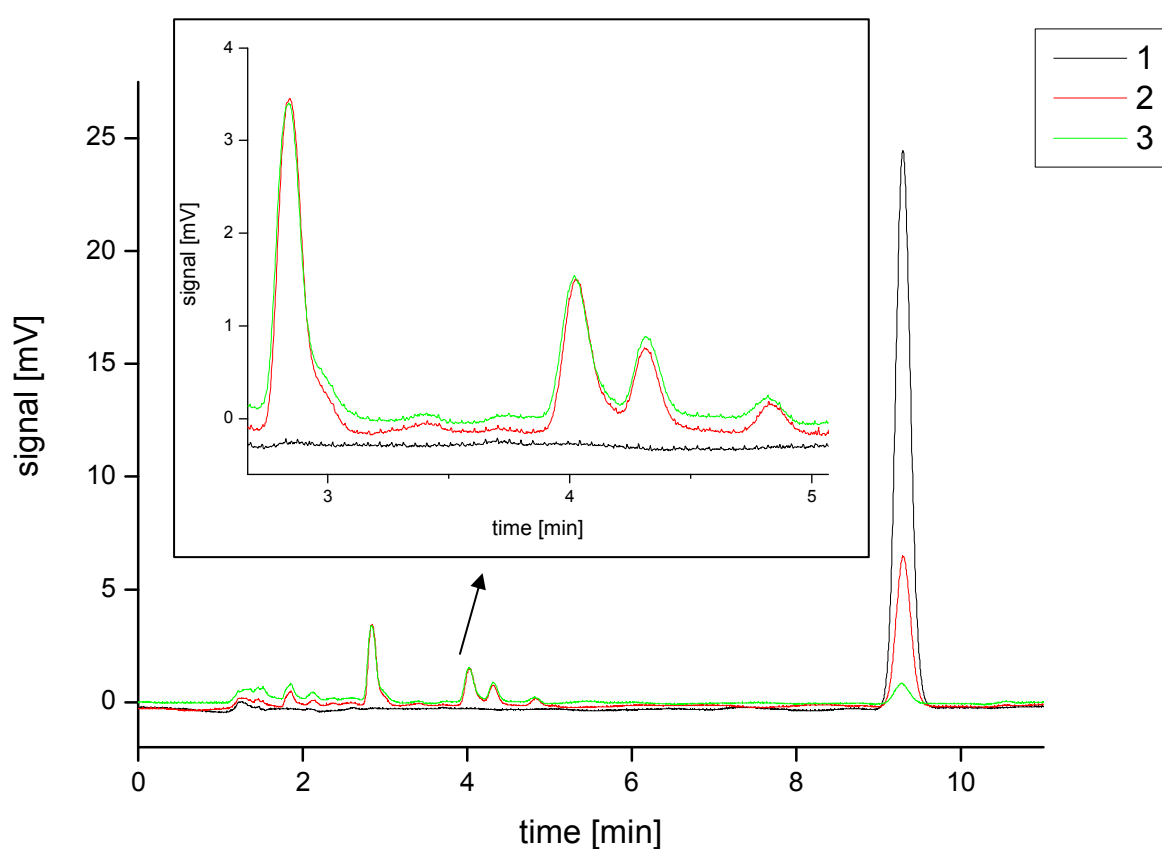


Figure 27 Chromatograms of NAP. Conditions: $c(\text{NAP}) = 2 \text{ mg/l}$, the flow rate was 1 ml/min , injection volume $25 \mu\text{l}$, the detector wavelength 280 nm , mobile phase composition - acetonitrile/ H_2O $50/50 \text{ (v/v)}$. Number 1 represents non irradiated NAP; number 2 represents irradiation for 30 s ; and number 3 represents irradiation for 70 s .

We can see that NAP degrades when exposed to UV light and even after 30 s of irradiation gives rise to photodegradation products. Further studies, however, need to be carried out in order to identify these newly formed structures.

Fig. 28 and Fig. 29 illustrate the photodegradation of inclusion complexes of NAP with CB7 and CD, respectively.

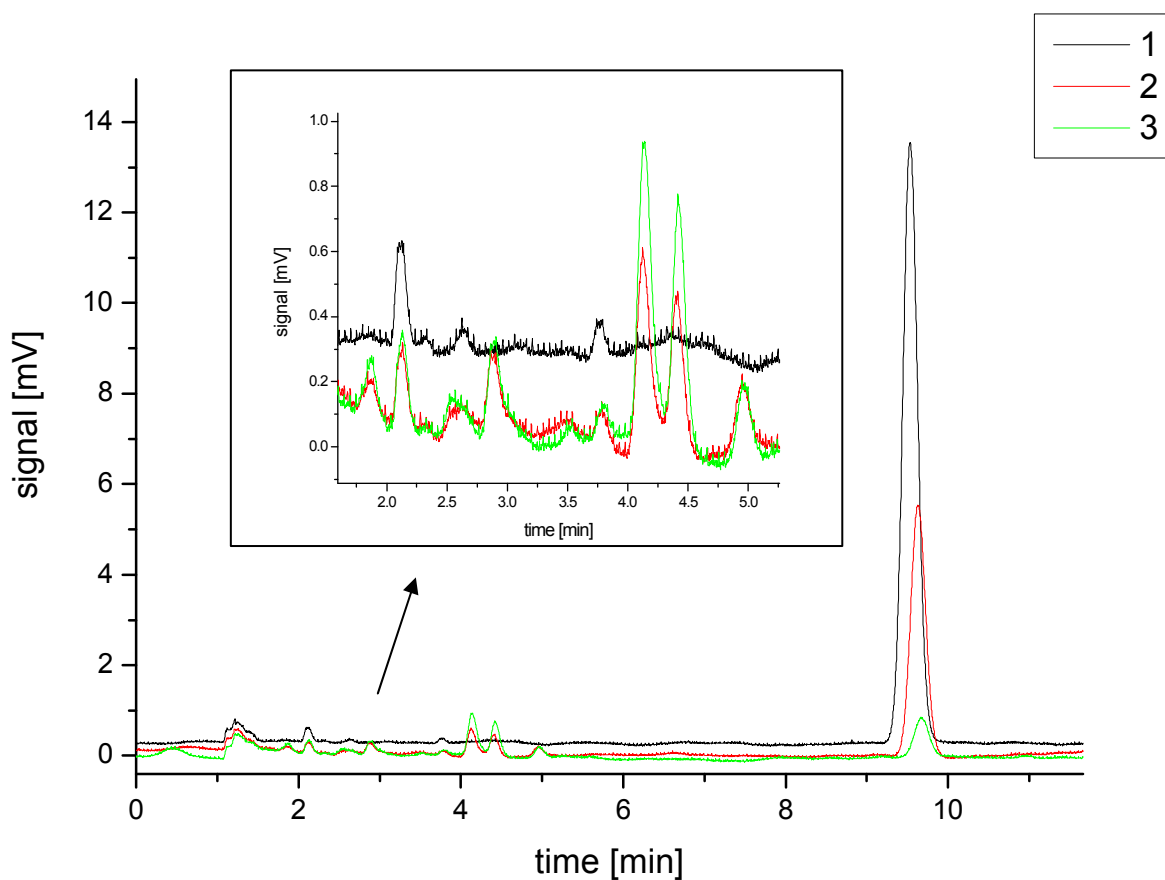


Figure 28 Chromatogram of inclusion complex of NAP with CB7. Conditions: $c(\text{NAP}) = 1 \text{ mg/l}$, $c(\text{CB7}) = 0.5 \text{ mg/l}$, for other conditions see Fig. 27 and Experimental. Number 1 represents non irradiated NAP; number 2 represents irradiation for 30 s; and number 3 represents irradiation for 70 s.

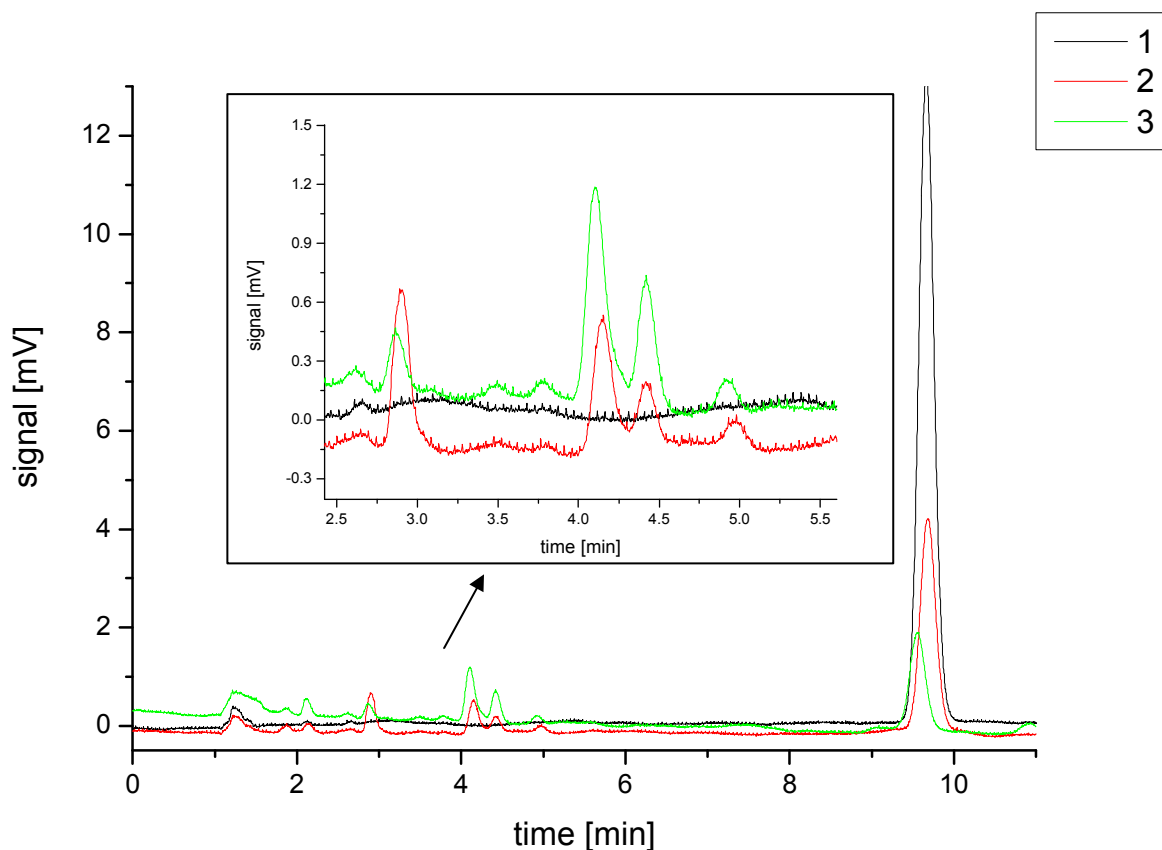


Figure 29 Chromatogram of inclusion complex of NAP with β -CD. Conditions: $c(\text{NAP}) = 1 \text{ mg/l}$, $c(\beta\text{-CD}) = 0.5 \text{ mg/l}$, for other conditions see Fig. 27 and Experimental. Number 1 represents non irradiated NAP; number 2 represents irradiation for 30 s; and number 3 represents irradiation for 70 s.

Analogically to free NAP, irradiation of both host-guest complexes led to degradation. Further studies, however, will have to be carried out in order to assign structures of degradation products.

5.4.2 Rate constant determination

In this method, we also aimed to obtain the rate constants of photodecomposition when evaluating the data, and compare them with results obtained by the previous method. As our analytes were successively irradiated, the dependences of the peak area on irradiation time were plotted followed by fitting by exponential function. Consequently, the dependences of natural logarithm of the peak area on the time of irradiation were plotted from which the slope value was found, thus the rate constant was determined.

The plot of area vs. time for NAP and the dependence of natural logarithm of area of the peak on irradiation time are shown in Fig. 30 and Fig. 31, respectively.

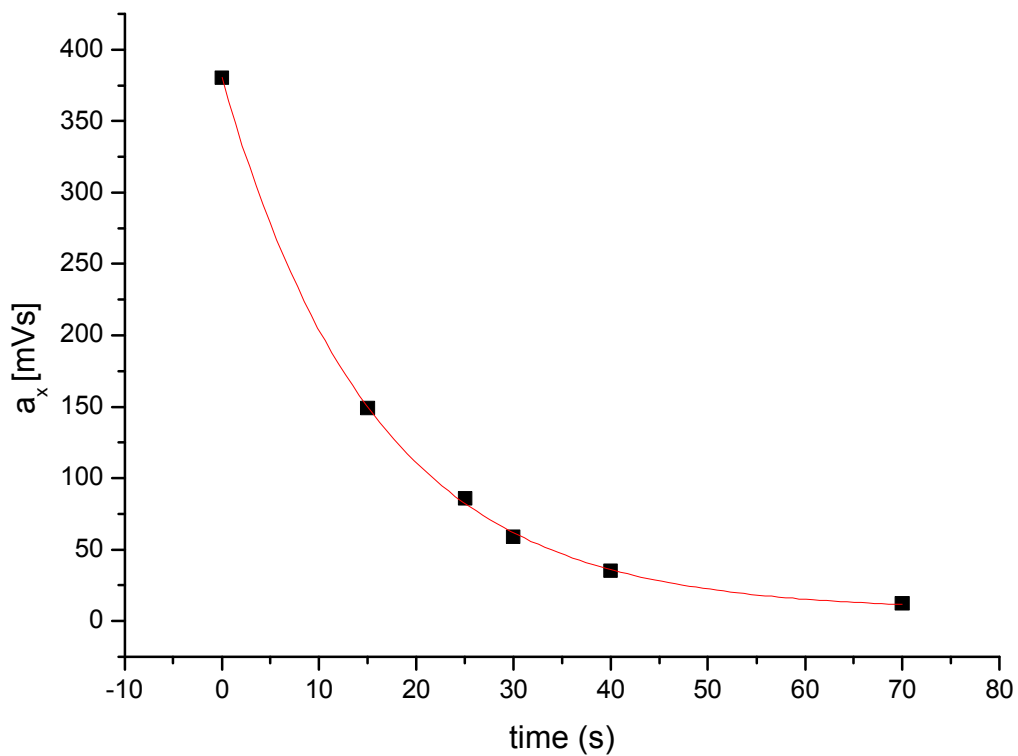


Figure 30 Dependence of area on irradiation time for NAP.

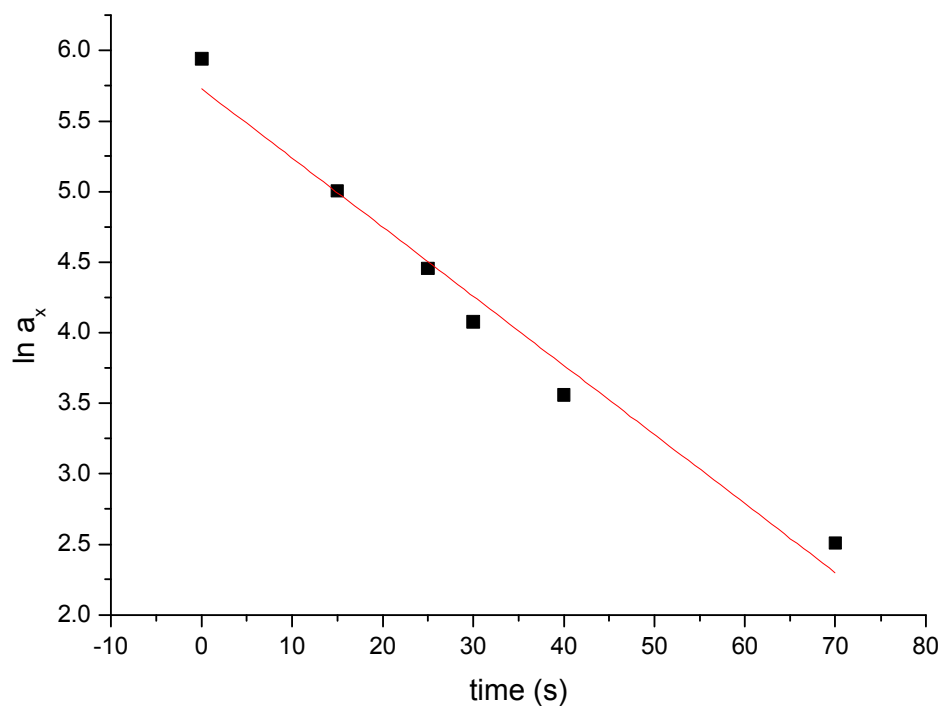


Figure 31 Dependence of natural logarithm of peak area on irradiation time for NAP.

Analogically, both graphs of inclusion complexes of NAP with CB7 and CD are presented in Fig. 32, Fig. 33, and Fig. 34, Fig. 35, respectively.

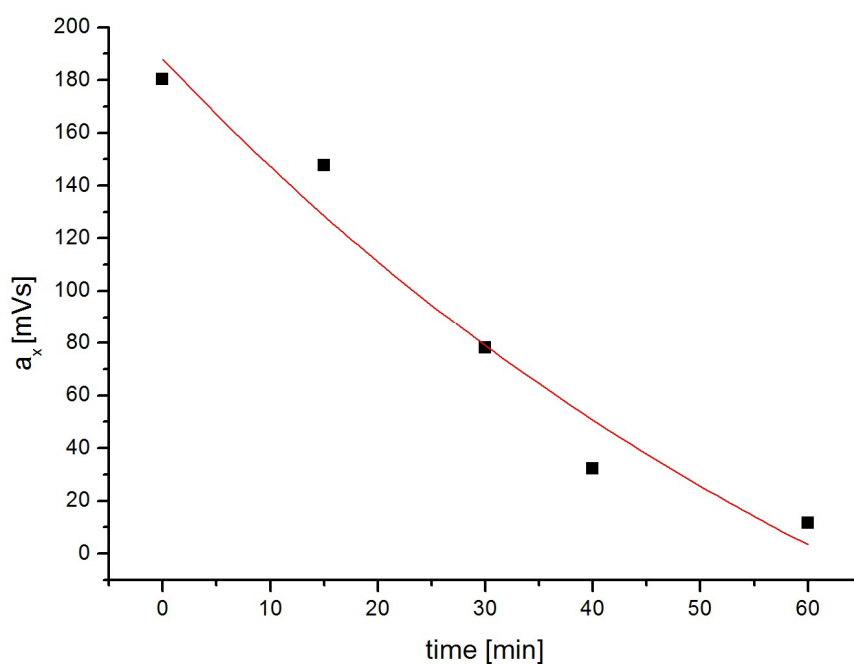


Figure 32 Dependence of peak area on irradiation time for NAP encapsulated into CB[7].

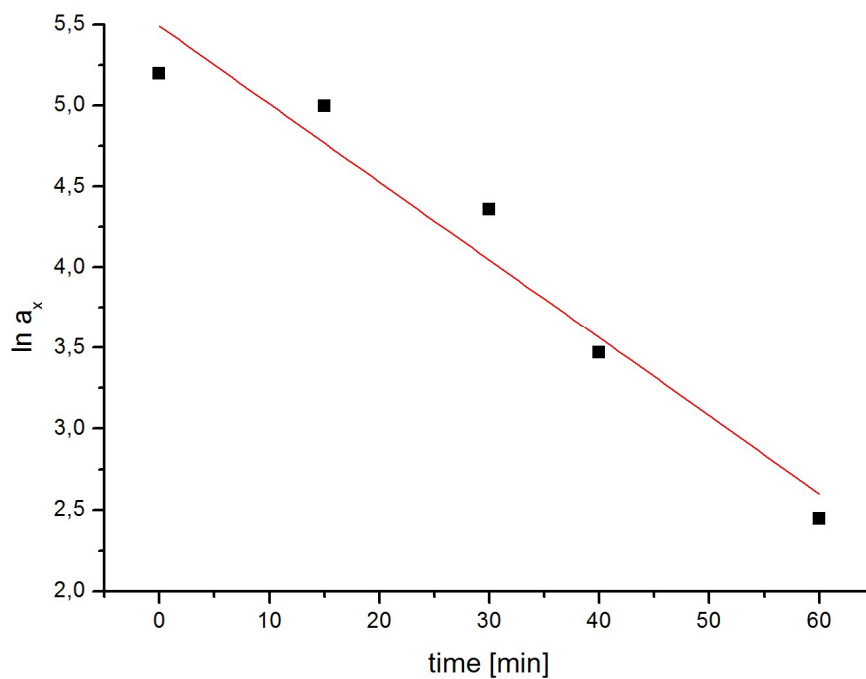


Figure 33 Dependence of natural logarithm of peak area on irradiation time for NAP encapsulated into CB[7].

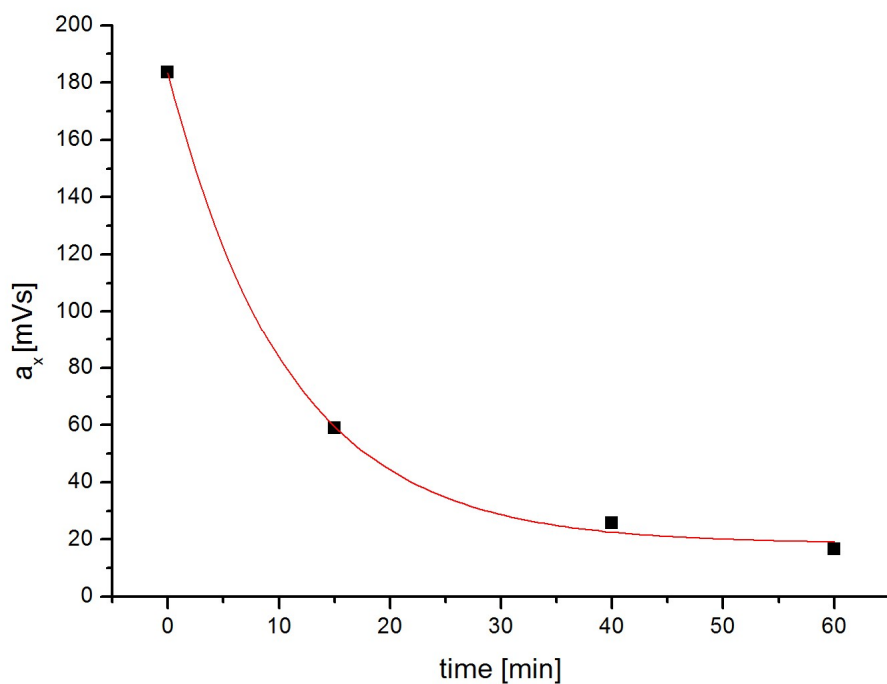


Figure 34 Dependence of peak area on irradiation time for NAP encapsulated into CB[7].

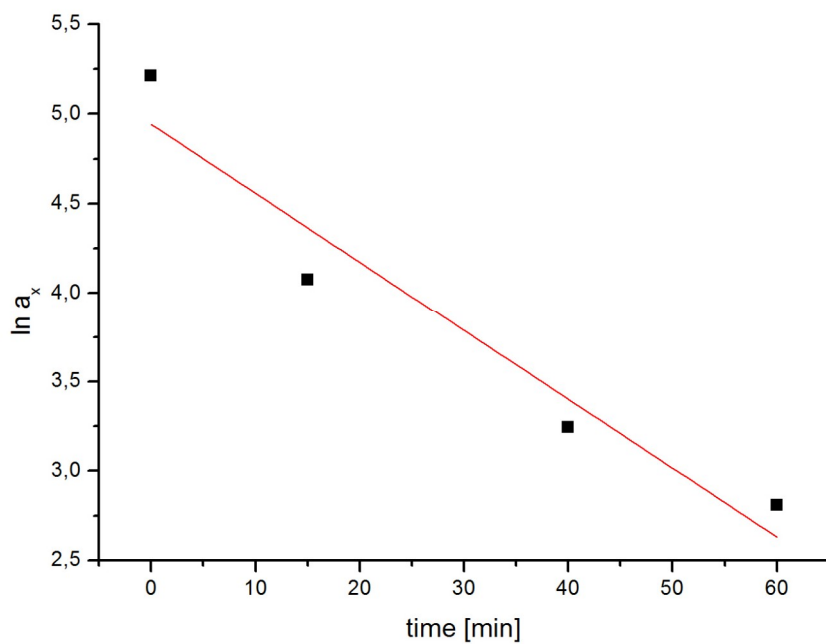


Figure 35 Dependence of natural logarithm of peak area on irradiation time for NAP encapsulated into CB[7].

Evaluated rate constants are presented in Tab. 7.

Table 7 Rate constants of pesticides degradation

Pesticide	k_x	R
NAAm	0.033	0.9892
NAAm@CB7	0.031	0.9820
NAAm@ β -CD	0.015	0.9664
NAAc	0.081	0.9863
NAAc@CB7	0,078	0,9805
NAAc@bCD	0,050	0,9997
Carb	0.051	0.9986
Carb@CB7	0.042	0.9891
Carb@bCD	0.028	0.9859
NAP	0.049	0.9879
NAP@CB7	0.048	0.9737
NAP@bCD	0.038	0.9677

Looking at the table we can say that NAAm, considering the degradation rate, falls apart in following order: $\text{NAAm} \geq \text{NAAm@CB7} > \text{NAAm@}\beta\text{-CD}$.

This tendency, however, is not maintained for other pesticides. In case of NAAc, fastest degrades NAAc@ β -CD, followed by the inclusion complex NAAc@CB7, and the last one is NAAc.

Considering Carb, the degradation trend is exactly the opposite of the NAAc, particularly the first to disintegrate comes Carb, followed by the inclusion complex Carb@CB7, and completed by the Carb@ β -CD.

NAP degrades analogically to Carb and its complexes.

Generally, the pesticides degrade faster when are not included within a molecular container. Given that the rate constants of cyclodextrin host-guest complexes are much higher than those of complexes with CBs, we can conclude that CDs stabilizes the pesticides more efficiently than CBs. It should be stated that the HPLC results of the rate

constants of photodegradation are based on less data than the results obtained by spectrometry. Therefore it is difficult to compare the final rate constant values. Nevertheless, some basic conclusions can be made at least for Carb, and NAP. Additional measurements should be performed.

6 Conclusions

The main aim of this work was to find out if the cucurbit[n]urils ($n = 7$ and 8) form any complexes with selected pesticides, namely 1-naphthylacetic acid, 1-naphthylacetamide, napropamide and carbaryl. Consequently, a study was carried out to find out if the CBs presence changes the photochemistry of the pesticides. The complexation effect on photodegradation of the pesticide was also compared with that of cyclodextrin as a host.

Direct injections were performed using the electrospray ionization mass spectrometry (ESI-MS), LC traces were acquired using both the liquid chromatography hyphenated with mass spectrometry (LC-MS) and high performance liquid chromatography (HPLC) coupled to UV/VIS detector. Spectrophotometric analysis also was carried out.

All the pesticides suffered photodegradation when irradiated with low pressure mercury lamp of 16 W of power ($\lambda = 254$ nm).

The electrospray ionization mass spectrometry technique proved, based on the m/z values, isotope distribution and fragmentations (MS^n), that all the pesticides form 1:1 (host:guest) complexes. 1-naphthylacetamide, napropamide and carbaryl create 1:2 (host:guest) complexes as well. It was also found out that CBs are readily detected and transformed into gas phase, containing ions H^+ , Na^+ or K^+ . We obtained a mixture of these ions in some cases. Under concentrations of cucurbiturils above $50 \mu M$ and low acid and salt concentrations ($< 10^{-5}$ M) aggregates can also be observed.

Using the HPLC method, the rate constants of photodegradation were acquired. Generally, when exposed to UV light, the free pesticides degrade faster than those within an inclusion complex of molecular container. It appears that cyclodextrin encapsulates the pesticides more efficiently than cucurbiturils which was also documented by the rate constants value.

LC measurements showed the decrease of absorbance as the compounds were irradiated and yielded new products. This also elucidates that these pesticides undergo photodegradation. Further studies, however, will be carried out in order to identify these products.

Rate constants of photodecomposition obtained from the spectrophotometric experiments also clarified the photodegradation aspects. The decomposition tendency of the naphthoxy pesticides, namely carbaryl and napropamide, was the same as determined by HPLC. Measurement conditions of 1-naphthylacetamide and 1-naphthylacetic acid should be further optimized to get consistent results.

References

1. Jeon, Y. M., Kim, J., Whang, D. Kim, K.: Molecular Container Assembly Capable of Controlling Binding and Release of Its Guest Molecules: Reversible Encapsulation of Organic Molecules in Sodium Ion Complexed Cucurbituril, *J. Am. Chem. Soc.*, **1996**, 118, 9790 – 9791.
2. Schneider, H-J., Kramer, R., Simova, S., Schneider, U.: Solvent and Salt Effects on Binding Constants of Organic Substrates in Macrocyclic Host Compounds. A General Equation Measuring Hydrophobic Binding Contributions, *J. Am. Chem. Soc.*, **1988**, 110, 6442 – 6448.
3. Márquez, C.; Hudgins, R. R.; Nau, W. M.: Mechanism of Host – Guest Complexation by Cucurbituril, *J. Am. Chem. Soc.*, **2004**, 126, 5806 – 5816.
4. Pozo, M. del, Hernández, L., Quintana, C.: A selective spectrofluorometric method for carbendazim determination in oranges involving inclusion-complex formation with cucurbit[7]uril, *Talanta*, **2010**, 81, 1542-1546.
5. Szejtli, J., Introduction and General Overview of Cyclodextrin Chemistry, *Chem. Rev.*, **1998**, 98, 1743-1753.
6. Del Valle, E. M. M.: Cyclodextrins and their uses: a review, *Process Biochem.*, **2004**, 39, 1033-1046.
7. Li, S., Purdy, W. C.: Cyclodextrins and Their Applications in Analytical Chemistry, *Chem. Rev.*, **1992**, 92, 1457-1470.
8. Connors, K. A.: The Stability of Cyclodextrin Complexes in Solution, *Chem. Rev.*, **1997**, 97, 1325-1357.
9. Uekama, K., Hirayama, F., Irie, T.: Cyclodextrin Drug Carrier Systems, *Chem. Rev.*, **1998**, 98, 2045-2076.
10. Lagona, J; Mukhopadhyay, P.; Chakrabarti, S.; Isaacs, L.: The Cucurbit[n]uril Family, *Angew. Chem. Int. Ed.*, **2005**, 44, 4844-4870.
11. Kim, K; Selvapalam, N.; Oh, D. H.: Cucurbiturils – a New Family of Host Molecules, *J. Incl. Phenom. Macro.*, **2004**, 50, 31-36.
12. Kim, K., Selvapalam, N., Ko, Y. H., Park, K. M., Kim, D., Kim. J.: Functionalized cucurbiturils and their applications, *Chem. Soc. Rev.*, **2007**, 36, 267-279.

-
13. Lee, J. W., Samal, S., Selvapalam, N., Kim, H-J., Kim, K.: Cucurbituril Homologues and Derivatives: New Opportunities in Supramolecular Chemistry, *Acc. Chem. Res.*, **2003**, 36, 621-630.
 14. Örgödoová, M.: Interaction of pesticides 1-naphthylacetic acid and 1-naphthylacetamide with cucurbit[7]uril and selected cyclodextrins, *Bachelor thesis*, Faculty of Science, Charles University in Prague, **2013**.
 15. Silva, J. P. Da; Jayaraj, N.; Jockusch, S.; Turro, N. J.; Ramamurthy, V.: Aggregates of Cucurbituril Complexes in the Gas Phase, *Org. Lett.*, **2011**, Vol. 13, No. 9.
 16. Turro, N. J.: *Modern Molecular Photochemistry*, University Science books, USA, 1991.
 17. Wayne, C.E; Wayne, R. P.: *Photochemistry*, Oxford Science Publications, 1996.
 18. Wayne, R.P: *Principles and Applications of Photochemistry*, Oxford Science Publications, USA, 1988.
 19. Rohatgi-Mukherjee, K. K.: *Fundamentals of Photochemistry*, New Age International, Calcutta, 1978.
 20. Fenn, J. B.; Mann, M.; Meng, C. K.; Wong, S. F.; Whitehouse, C. M.: Electrospray Ionization for Mass-Spectrometry of Large Biomolecules, *Science*, **1989**, 246, 64-71.
 21. Hoffman E. de, Charette J., Stroobant V.: *Mass Spectrometry – Principles and Applications*, John Wiley & Sons, Chichester, 1999.
 22. Barker, J.: *Mass Spectrometry: Analytical Chemistry by Open Learning*, 2nd ed.; Wiley, 1999; p. 532.
 23. Fenn, J. B.: Electrospray Wings for Molecular Elephants (Nobel Lecture), *Angew. Chem. – Int. Edit.*, **2003**, 42, 3871-3894.
 24. Dass, Ch.: *Fundamentals of Contemporary Mass Spectrometry*, Wiley, USA, 2007.

-
25. Ekman R., Silberring J., Westman-Brinkmalm A. M., Kraj A.: Mass Spectrometry – Instrumentation, Interpretation, and Applications, John Wiley & Sons, Hoboken, 2009, p. 372.
 26. Niessen W. M. A.: Liquid Chromatography-Mass Spectrometry, CRC Press, New York, 2006.
 27. HCT ultra, User Manual, Bruker Daltonics, 2006.
 28. http://holcapek.upce.cz/teaching/MS_2012/MS045_Hmotnostni_analyzatory.pdf, cited 1. 6. 2012
 29. Soler C., James, K. J., Pico, Y.: Capabilities of Different Liquid Chromatography Tandem Mass Spectrometry Systems in Determining Pesticide Residues in Food – Application to Estimate their Daily Intakes, *J. Chromatogr. A.*, **2007**, 1157, 73-84.
 30. Liska, I., Slobodnik, J.: Comparison of gas and liquid chromatography for analysing polar pesticides in water samples, *J. Chromatogr. A*, **1996**, 733, 235-258.
 31. Braithwaite, A., Smith, F. J.: Chromatographic methods, Blackie Academic&Professional, Glasgow, **1996**.
 32. Štulík, K. *et al.*: Analytické separační metody, Karolinum, Praha, **2004**.
 33. Churáček, J., Jandera, P.: Úvod do vysokoúčinné kapalinové chromatografie, SNTL, Praha, **1984**.
 34. Hemström, P., Irgum, K.: Hydrophilic interaction chromatography, *J. Sep. Sci.*, **2006**, 29, 1784-1821.
 35. Churáček, J. *et al.*: Analytická separace látek, SNTL, Praha, **1990**.
 36. Dong, M. W.: Modern HPLC for practicing scientists, John Wiley and sons, Inc., **2006**.
 37. Opekar, F., Jelínek, I., Rychlovský, P., Plzák, Z.: Základní analytická chemie, Karolinum, **2007**.
 38. Douša, M.: Typy detektorů v HPLC, <http://www.hplc.cz/Teorie/detectors.html>, cited on 20th April 2013.

-
39. Cui, L.E., Yang, H.: Accumulation and residue of napropamide in alfalfa (*Medicago sativa*) and soil involved in toxic response, *J. Hazard. Mater.*, **2011**, 190, 81-86.
 40. Mauriz, E., Calle, A., Abad, A., Montoya, A., Hildebrandt, A., Barceló, D., Lechuga, L. M.: Determination of carbaryl in natural water samples by a surface plasmon resonance flow-through immunosensor, *Biosens. Bioelectron.*, **2006**, 21, 2129-2136.
 41. Buser, H.R., Müller, M.D.: Isomer-Selective and Enantiomeric Determination of DDT and Related Compounds Using Chiral High-Resolution Gas Chromatography/Mass Spectrometry and Chiral High-Performance Liquid Chromatography, *Anal. Chem.*, **1995**, 67, 2691-2698.
 42. Granby, K., Andersen, J.H., Christensen, H.B.: Analysis of pesticides in fruit, vegetables and cereals using methanolic extraction and detection by liquid chromatography-tandem mass spectrometry, *Anal. Chim. Acta*, **2004**, 520, 165-176.
 43. Abad, A., Moreno, M.-J., Pelegrí, R., Martínez, M.-I., Sáez, A., Gamón, M., Montoya, A.: Monoclonal Enzyme Immunoassay for the Analysis of Carbaryl in Fruits and Vegetables without Sample Cleanup, *J. Agric. Food Chem.*, **2001**, 49, 1707-1712.
 44. Abad, A., Moreno, M.-J., Pelegrí, R., Martínez, M.-I., Sáez, A., Gamón, M., Montoya, A.: Determination of carbaryl, carbofuran and methiocarb in cucumbers and strawberries by monoclonal immunoassays and high-performance liquid chromatography with fluorescence detection. An analytical comparison, *J. Chromatogr. A*, **1999**, 833, 3-12.
 45. Gou, Y., Eisert, R., Pawliszyn, J.: Automated in-tube solid-phase microextraction high performance liquid chromatography for carbamate pesticide analysis, *J. Chromatogr. A*, **2000**, 873, 137-147.
 46. Skládal, P., Nunes, G.S., Yamanaka, H., Ribeiro, M. L.: Detection of Carbamate Pesticides in Vegetable Samples Using Cholinesterase-Based Biosensors, *Electroanal.*, **1997**, 9, No. 14, 1083-1087.

-
47. Fu, L., Liu, X., Hu, J., Zhao, X., Wang, H., Wang, X.: Application of dispersive liquid-liquid microextraction for the analysis of triazophos and carbaryl pesticides in water and fruit juice samples, *Anal. Chim. Acta.*, **2009**, 632, 289-295.
48. Biswas, P.K., Pramanik, S.K., Mitra, S.R., Bhattacharyya, A.: Persistence of Napropamide in/on Tea Under North-East Indian Climatic Condition, *Bull Environ Contam Toxicol*, **2007**, 79, 566-599.
49. Li, Y.-N., Wu, H.-L., Qing, X.-D., Nie, Ch.-Ch., Li, S.-F., Yu, Y.-J., Zhang, S.-R., Yu, R.-Q.: The maintenance of the second-order advantage: Second-order calibration of excitation-emission matrix fluorescence for quantitative analysis of herbicide napropamide in various environmental samples, *Talanta*, **2011**, 85, 325-332.
50. Zhang, R., Cui, J., Zhu, H.M., Yang, H.: Effect of Dissolved Organic Matters on Napropamide Availability and Ekotoxicity in Rapeseed (*Brassica napus*), *J. Agric. Food Chem.*, **2010**, 58, 3232-3240.
51. Qing, X.-D., Wu, H.-L., Li, Y.-N., Nie, Ch.-Ch., Wang, J.-Y., Zhu, S.-H., Yu, R.-Q.: Simultaneous determination of pre-emergence herbicides in environmental samples using HPLC-DAD combined with second-order calibration based on self-weighted alternating trilinear decomposition algorithm, *Anal. Methods*, **2012**, 4, 685-692.
52. Tang, B., Liu, W.-L., Wang, Y., Chen, Z.-Z.: Studies on the supramolecular interaction between napropamide and β -cyclodextrin by spectrofluorimetry and its analytical application, *Anal. Chim. Acta*, **2004**, 509, 145-150.
53. Da Silva, J.P., Bastos, E.V., Ferreira, L.F.V., Weiss, R.G.: Surface photochemistry of the herbicide napropamide. The role of the media and environmental factors in directing the fates of intermediates, *Photochem. Photobiol. Sci.*, **2008**, 7, 69-75.
54. Chang, L.-L., Giang, B. Y., Lee, K.- S., Tseng, Ch. K.: Aqueous Photolysis of Napropamide, *J. Agric. Food Chem.*, **1991**, 39, 617-621.

55. Carretero, A., S., Blanco, C., C., Gutiérrez, A.,F.: Experimental Studies of the Factors That Influence 1-Naphthaleneacetamide Determination by Micelle-stabilized Room-temperature Phosphorescence, *Analyst*, **1997**, 122, 563-566.
56. Vilchez, J. L., Blanc, R., Navalón, A.: Simultaneous spectrofluorimetric determination of 1-naphthylacetic acid and 1-naphthaleneacetamide in commercial formulations and soil samples, *Talanta*, **1997**, 45, 105-111.
57. Pulgarín, J.,A.,M., López, P., F., Bermejo, L.,F.,G., Alfonso, F.,M.: Fast Kinetic Determination of 1-Naphthylacetic Acid in Commercial Formulations, Soils, and Fruit Samples Using Stopped-Flow Posphorimetry, *J. Agric. Food Chem.*, **2003**, 51, 6380-6385.
58. Sigrist, R., Temperli, A., Hurter, J.: A Fluorometric Method for the Determination of Residues of 1-Naphthaleneacetamide and 1-Naphthaleneacetic Acid on Apples, *J. Agr. Food Chem.*, **1974**, 22, 568-570.
59. Navalón, A., Blanc, R., Vilchez, J., L.: Determination of 1-Naphthylacetic Acid in Commercial Formulations and Natural Waters by Solid-Phase Spectrofluorimetry, *Mikrochim. Acta*, **1997**, 126, 33-38.